

See discussions, stats, and author profiles for this publication at: <https://www.researchgate.net/publication/362669922>

# Impacts of uncertainty in building envelope thermal transmittance on heating/cooling demand in the urban context

Article in Energy and Buildings · August 2022

DOI: 10.1016/j.enbuild.2022.112363

CITATIONS

5

READS

245

5 authors, including:



Zhaoru Liu

Tsinghua University

5 PUBLICATIONS 71 CITATIONS

[SEE PROFILE](#)



Xin Zhou

Southeast University (China)

64 PUBLICATIONS 1,379 CITATIONS

[SEE PROFILE](#)



Wei Tian

Tianjin University of Science and Technology

96 PUBLICATIONS 2,910 CITATIONS

[SEE PROFILE](#)



Xue Liu

Tsinghua University

12 PUBLICATIONS 140 CITATIONS

[SEE PROFILE](#)

Some of the authors of this publication are also working on these related projects:



ASHRAE Multidisciplinary Task Group on Occupant Behavior in Buildings [View project](#)



International Energy Agency Energy in Buildings and Communities Programme, Annex 66, Definition and Simulation of Occupant Behavior in Buildings [View project](#)

1           **Impacts of uncertainty in building envelope thermal transmittance on**  
2           **heating/cooling demand in the urban context**

3           Zhaoru Liu<sup>a</sup>, Xin Zhou<sup>b</sup>, Wei Tian<sup>c</sup>, Xue Liu<sup>a</sup>, Da Yan<sup>a,\*</sup>

4           <sup>a</sup>*Building Energy Research Center, School of Architecture, Tsinghua University, Beijing 100084, China*

5           <sup>b</sup>*School of Architecture, Southeast University, Nanjing 210096, Jiangsu, China*

6           <sup>c</sup>*College of Mechanical Engineering, Tianjin University of Science and Technology, Tianjin, 300222, China*

---

7           **Abstract**

8         Urban building energy modeling (UBEM) is a promising tool to evaluate building energy consumption at high  
9         temporal-spatial resolution at urban scale. However, state-of-the-art UBEMs use identical building envelope thermal  
10        transmittance according to design specifications in model characterization, which neglects the uncertainty in U-values  
11        of the building stock. To evaluate the impacts of uncertainty in U-values on heating/cooling demand at the urban  
12        scale, this study proposes a physics-based model of building envelope thermal transmittance to generate the U-value  
13        distributions of building stocks. Diversified U-values were assigned to buildings according to the building age, while  
14        identical initial U-values in the design served as a baseline. The impact of uncertainty in building envelope U-  
15        values was assessed by comparing the heating/cooling demand simulated under different U-value distributions, taking  
16        33,222 residential buildings in Beijing as a case study. The results showed that, considering uncertain physical factors,  
17        thermal transmittance followed a right-skewed distribution, which led to an increase in the heating/cooling demand of  
18        the building stock. The annual total heating/cooling demand increased by 26% and 13%, respectively. The diversity  
19        in the heating/cooling demand intensity of the building stock was enhanced when more causes of uncertainty were  
20        considered, which was more evident in the building stock with a small range of building age or heating demand  
21        intensity. Therefore, it is advisable to consider the uncertainty in the building envelope thermal transmittance in  
22        UBEM simulations for energy evaluation and planning at the district or urban scale.

23        **Keywords:** Urban building energy modeling, Uncertainty analysis, Building envelope, Thermal transmittance,  
24        Residential buildings, Stochastic modeling.

---

25           **1. Introduction**

26         The building sector accounts for approximately 35% of the total global energy consumption and 38% of the  
27         total global energy-related CO<sub>2</sub> emissions[1], with buildings in urban areas playing a dominant role. In the U.S.  
28         and European Union (EU), urban building stocks in urban areas are responsible for up to 70% of primary energy

---

\*Corresponding authors

Email address: [yanda@tsinghua.edu.cn](mailto:yanda@tsinghua.edu.cn) (Da Yan)

29 consumption [2, 3]. In China, urban building stocks consumed 78% of commercial energy in 2019 [4]. Therefore,  
30 building energy conservation at an urban scale is a growing concern [5]. Analyzing energy consumption at the urban  
31 scale is important and can support energy transition practices and energy policy formulation.

32 *1.1. Urban building energy modeling*

33 Urban building energy Modelling (UBEM) is a method for quantifying operational energy demand in an urban  
34 context [6], and the approaches of UBEM are classified into two categories: top-down and bottom-up[7]. The bottom-  
35 up physics-based approach is a relatively nascent field of the UBEM [8]. Physics-based building energy models of  
36 urban building stock are automatically generated by UBEM platforms based on multi-source urban building data,  
37 and the building performance is simulated by the simulation engine. The energy demand of the building stock can  
38 be calculated with hourly or sub-hourly time steps, which supports building benchmarking analyses[9], scenario  
39 evaluation [10], energy pattern analyses [11], policy measures development for building stocks [12] and other specific  
40 analyses. To date, various UBEM platforms have been proposed in numerous studies [13].

41 Reflecting the diversity of building stocks is one of the main challenges of UBEMs, which makes them more  
42 difficult than the simple summation of building energy models (BEMs) [14]. However, owing to the lack of available  
43 data and the difficulty in quantifying data with uncertainty, most UBEMs are characterized by simplified deterministic  
44 approaches. BEMs are categorized based on building typology or cluster analysis [15, 16], and are defined by referring  
45 to the default templates, standards, or open project data[17].

46 Probabilistic characterization of building archetypes is an attempt to improve the fidelity of UBEMs. Some char-  
47 acteristics with high uncertainty are treated stochastically, such as occupant schedules [18], behavior [19, 20], air  
48 change rate [21], window-to-wall ratio [22] and thermal properties[23]. In some case studies, the probabilistic dis-  
49 tribution of occupant-related parameters was considered, and the uncertain parameters were calibrated based on the  
50 Bayesian calibration method [23, 24, 25]. To consider the correlation among UBEM characteristics, a probabilistic  
51 building characterization method was proposed to estimate multivariate distributions based on known data [26]. How-  
52 ever, only a few probabilistic methods have been applied to the current UBEM platforms. In the platforms considering  
53 probabilistic distributions of parameters, the parameters are determined by common probability distribution models,  
54 which may be discrepant from those in real building stocks owing to the lack of consideration of the driving forces of  
55 the distribution.

56 *1.2. Uncertainty of building envelope thermal transmittance*

57 The building envelope has an important effect on the thermal performance of a building, and the thermal trans-  
58 mittance is a dominant parameter with high uncertainty [27]. High uncertainty may be introduced into the building  
59 envelope thermal transmittance by the presence of air cavities [28], moisture content [29], construction layering and  
60 material quality [30]. Although buildings are designed and built according to the design standards at that time, there

61 may be gaps between the thermal performance of the existing building stock and design performance, owing to pro-  
62 longed exposure to the environment, as well as different levels of construction and maintenance. Therefore, after  
63 building are designed and constructed, the operational stage may introduce uncertainty in the thermal performance of  
64 building envelopes installed on building surfaces.

65 Numerous studies have been conducted on the changes or uncertainty in the thermal performance of building  
66 envelopes [31], and the deterioration of building envelopes with time has been verified in both experiments and  
67 in situ measurements. Several experimental studies have focused on the uncertainty in the thermal properties of  
68 insulation boards made of the same type of material. The uncertainty in the thermal conductivity of common types  
69 of insulation materials was quantified using conductivity measurements from European national laboratories [32].  
70 Several studies have tested performance deterioration under laboratory conditions. Accelerated aging test methods  
71 have been developed and applied in the tests of polyurethanes [33, 34] and vacuum insulation panels [35, 36] to predict  
72 the long-term thermal performance. Long-term hygrothermal behavior under constant conditions [37] and periodic  
73 freezing-thawing processes [38] have also been studied. Other experimental studies tested thermal performance of  
74 mock-up walls. A test procedure by hot box method was presented to assess the overall thermal performance of  
75 inhomogeneous mock-up walls [39]. As for in situ measurements, non-destructive techniques for diagnosis of existing  
76 buildings were reviewed in [40]. Some studies monitored the multi-year aging effect of building envelopes in the  
77 field [41] or tested insulation samples from an existing building to quantify any changes in the thermal properties of  
78 the material [42]. Heat flow meter measurement techniques were used for performance assessment on brick or stone  
79 masonries [30, 28]. A non-destructive monitoring method combined with dynamic simulations was applied to analyze  
80 the hygrothermal behavior of historic wall [29]. Besides, thermography has been used to detect thermal anomalies in  
81 building envelopes [43]. Using aerial thermography, the measured U-values showed a large difference from the values  
82 from the design specifications, and the calibrated U-values improved the fidelity of the BEM[44].

83 In summary, existing research on the changes or uncertainty in the thermal performance of building envelopes  
84 mainly focuses on experiments of the thermal performance of materials or in situ measurements of the deterioration  
85 of building envelopes of a case study building. However, the comprehensive thermal performance of a building  
86 envelope may be affected by more human factors, such as the quality and techniques in production and installation,  
87 as well as damage to insulation systems. In addition, experiments and in situ measurements may not be suitable for  
88 characterizing the entire building stock.

89 As for applications in UBEMs, few studies have considered the uncertainty of the building envelope thermal  
90 transmittance. For most current platforms, deterministic approaches are adopted in building envelope characterization,  
91 grouping buildings of similar ages together, and setting U-values referring to standards, codes, or design specifications  
92 [45]. In other studies that considered the uncertainty of building envelope thermal transmittance, simplified probabilis-  
93 tic distributions were used to describe the characteristics of building envelopes, such as a normal distribution[24, 46],  
94 uniform distribution [23], or discrete distribution [47]. In addition, because existing research mainly focuses on pa-  
95 rameter calibration, the analysis of the specific impact on the characteristics of the heating/cooling demand is not

96 sufficient.

97 In this study, the causes of uncertainty were investigated and divided into two main categories as shown in Fig.1.  
98 Although buildings built with the same vintage are considered to have identical initial U-values in design, the thermal  
99 performance of the building envelope may be diversified after years of service. The terminology *discrepancy* and  
100 *stochasticity* was used to describe them. Discrepancy is used to describe the differences between the average U-values  
101 of buildings built in a particular year and the initial U-values. Owing to the aging processes, building envelopes  
102 may deteriorate, leading to higher U-values, and the deterioration is relevant to building age; that is, the U-values of  
103 buildings built in 2000 and 2008 might be different because of the different periods of aging processes, although they  
104 were designed to meet the requirements of the same standard. Stochasticity is used to describe random variations  
105 in the U-values of buildings built in the same year. The thermal performance of the building envelope can also be  
106 influenced by the level of management and maintenance, which introduces uncertainty into buildings built in the  
107 same year. Therefore, two possible causes of uncertainty in building envelope thermal transmittance were selected to  
108 investigate the impacts on urban heating/cooling demand.

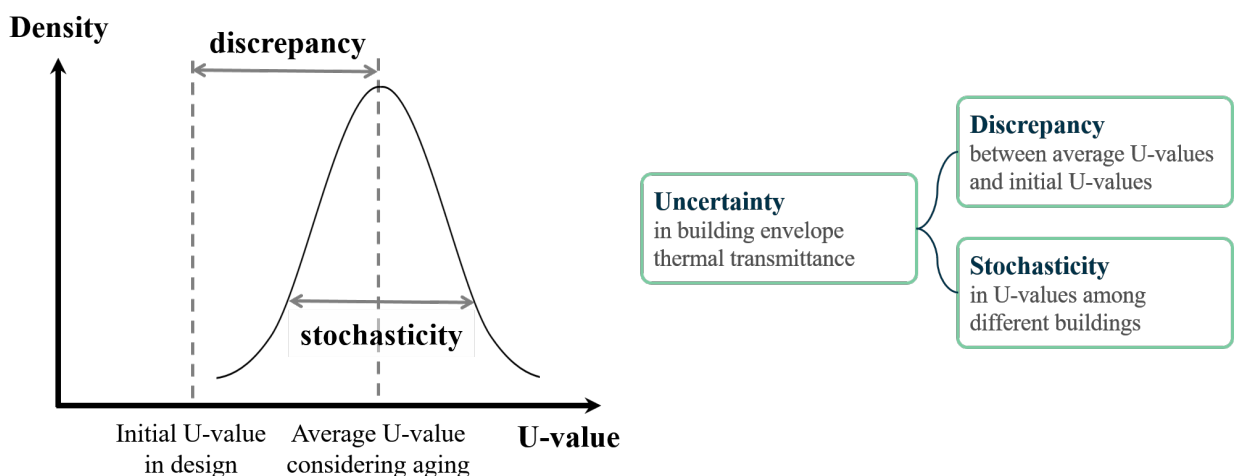


Figure 1: Possible causes of uncertainty in building envelope thermal transmittance of urban building stock and the illustration.

109 *1.3. Aim and research questions*

110 According to the above analysis, state-of-the-art UBEM research assigned limited U-values to buildings according  
111 to design specifications, which did not address the uncertainty of building envelope thermal transmittance at the urban  
112 scale, including both the discrepancy in the average level with time and stochasticity among different buildings. The  
113 gap between the design U-values and those in the real urban building stock may cause misestimation of heating/cooling  
114 demand. However, the impacts of the gap on heating/cooling demand of urban building stock remains unclear. The  
115 objective of this study is to better understand the impact of uncertainty in building envelope thermal transmittance

116 on heating/cooling demand of urban building stock. For this purpose, a physics-based approach was proposed to  
117 generate diversified building envelope thermal transmittances, and was employed for a residential building stock  
118 in Beijing. Then, a UBEM tool was used to simulate the heating/cooling demand of each building, considering  
119 different distributions of thermal transmittance. These results were then analyzed in relation to the **main research**  
120 **question:** What are the impacts of considering the uncertainty in building envelope thermal transmittance on UBEM  
121 simulations?

122 To address the main question, the following three concrete questions are addressed in a case study:

- 123 • (Q1) Is the status quo, the U-value model assuming the real U-values are the same as the initial U-values in  
124 design, an accurate model to represent the actual state of building stocks? How to quantitatively model U-values  
125 of a building stock considering uncertainty?
- 126 • (Q2) What are the differences in the impacts of uncertainty in U-values on heating/cooling demand in different  
127 dimensions of time (annual, diurnal or hourly) and space (individual building or urban scale)?
- 128 • (Q3) What is the sufficient fidelity for building envelope U-value models for different UBEM simulation pur-  
129 poses and contexts, i.e. the suitability of the different U-value models?

130 The answers to these questions could provide a better understanding of the mechanism of UBEM, and urban  
131 managers and urban energy analysts could use the information to establish UBEM in the appropriate approach for  
132 different contexts and purposes of UBEM.

133 To answer (Q1), the uncertainty of building envelope thermal transmittance of buildings has been divided into two  
134 effects: (1) the discrepancy between the average levels and the initial U-values in design, and (2) the stochasticity  
135 in thermal transmittance among different buildings. Models of building envelope thermal transmittance considering  
136 discrepancy and stochasticity were proposed based on the mathematical modeling of physical factors affecting U-  
137 values.

138 To address (Q2), three models were set up for comparative analysis: the status-quo approach (base-uniform), the  
139 approach considering discrepancy (aged-uniform), and the approach considering both discrepancy and stochasticity  
140 (aged-diverse). The U-value distributions generated by the three models were employed in UBEM characterization to  
141 simulate the heating/cooling demand of the building stock. The annual, diurnal, and hourly heating/cooling demands  
142 at the urban scale and the distributions of demand intensity at the building level in the three approaches were analyzed.  
143 The simulation results of the three approaches were compared to explore the different impacts of uncertainty in U-  
144 values on the heating/cooling demand.

145 To answer (Q3), the results of the three proposed models were investigated from the perspective of UBEM pur-  
146 poses and contexts. Thorough investigations of the results highlight the circumstances under which the discrepancy  
147 or stochasticity can be neglected, and the thermal transmittance of the urban building stock can be substituted with a  
148 simpler model. Such investigations also provide insights into situations in which uncertainty is highly influential on

149 the results.

150 The remainder of this study is structured as follows. Section 2 illustrates the building envelope U-value models,  
151 urban building energy modeling, and comparison method. Physics-based approaches to generate diversified thermal  
152 transmittance of building envelopes are introduced from the aspects of physical factors with uncertainty and the  
153 corresponding mathematical models. The workflow of UBEM and the comparison method are introduced. In Section  
154 3, the characteristics of the urban building stock are specified, such as building geometry and year of construction.  
155 The results are presented in section 4. The distributions of the building envelope thermal transmittance generated by  
156 these approaches were analyzed. The impacts on heating/cooling demand are analyzed in different dimensions: the  
157 annual, diurnal, or hourly demand, and building level or urban scale. Section 5 is followed by the conclusions in  
158 Section 6.

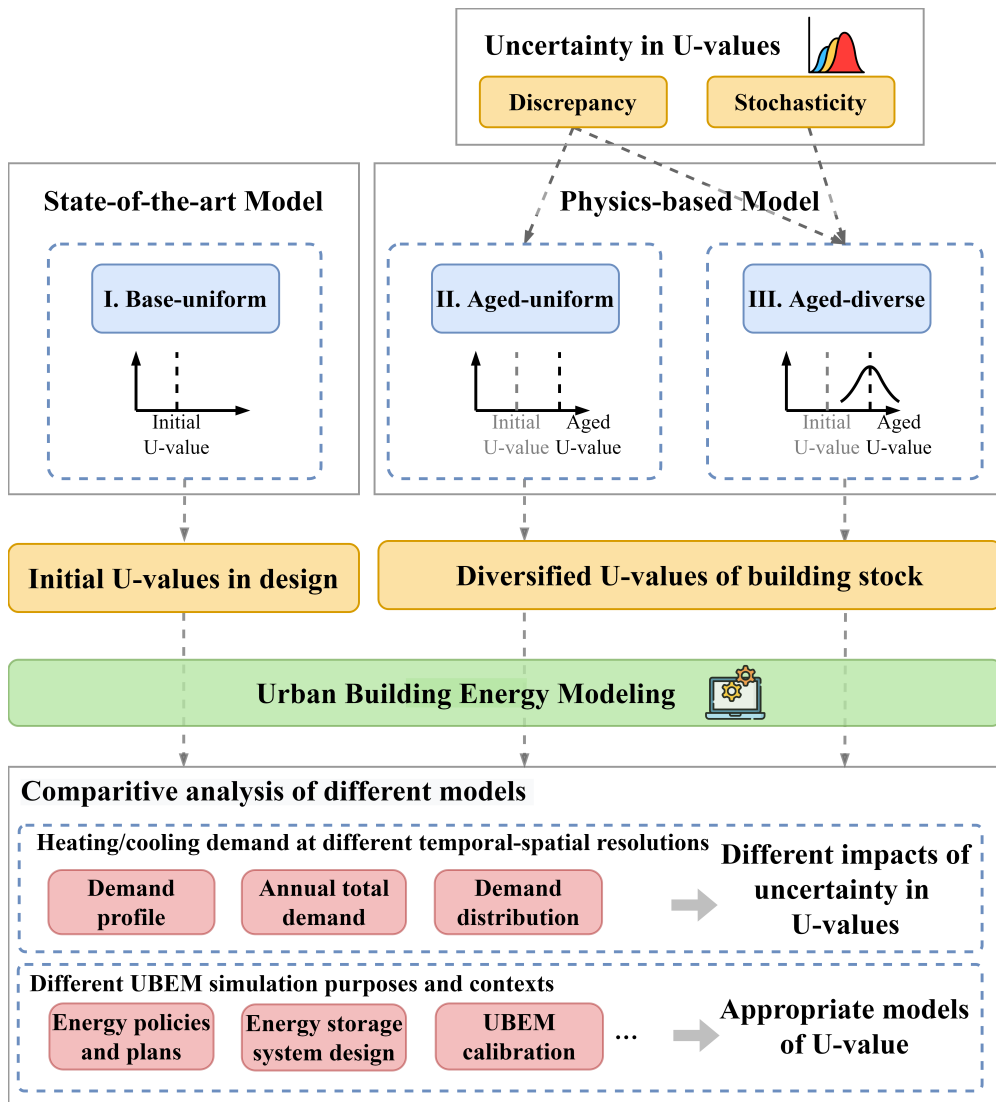


Figure 2: Technical approach of this research.

159 **2. Methodology**

160 The technical approach used in this study is illustrated in Fig.2. This research proposed two physics-based models  
161 of building envelope thermal transmittance to consider uncertainty, including the discrepancy between the actual  
162 average U-values and initial U-values, as well as the stochasticity in U-values among different buildings. The status-  
163 quo model was also chosen as the baseline. The U-values of the building stock were generated using the three models  
164 and were employed in urban building energy modeling. Heating/cooling demands calculated by different models  
165 were summarized and compared at different temporal-spatial resolutions to assess the different impacts of uncertainty  
166 in building envelope thermal transmittance. In addition, different UBEM simulation purposes and contexts were  
167 explored, and appropriate U-value models were selected under different circumstances. The methodology consists of  
168 three main parts: (1) a physics-based model of building envelope thermal transmittance, (2) urban building energy  
169 simulation with a proposed UBEM tool, and (3) a comparison method. The three parts are as follows.

170 *2.1. Physics-based model of building envelope thermal transmittance*

171 The physics-based model of building envelope thermal transmittance aims to reflect the change in the perfor-  
172 mance of the building envelope in the actual environment and quantify the difference from the initial values in the  
173 design. However, models focusing on in-situ changes in the building envelope thermal transmittance have rarely been  
174 proposed. In this study, two common physical factors that affect the U-value were studied and quantified using math-  
175 ematical models. Physics-based models can reflect the uncertainty in the building envelope thermal transmittance to  
176 a certain extent and serve as a starting point for subsequent heating/cooling demand analysis. More realistic models  
177 require more knowledge of failure analysis and the mechanism of the building envelope thermal performance. In the  
178 following sections, the physical factors affecting the U-value, associated mathematical models, and models of building  
179 envelope thermal transmittance are described.

180 *2.1.1. Physical factors affecting U-value*

181 In the status-quo UBEM, the U-values of the building envelopes are characterized based on the design specifica-  
182 tions or standards. However, the thermal performance of the building envelope may change over time during the long  
183 service period of a building. The performance of thermal insulation is easily affected in the operation stage, the longest  
184 stage of the building life cycle [48], which plays a dominant role in the building envelope thermal transmittance. In-  
185 sulation materials may affect the thermal performance of building envelopes from two aspects: (1) deterioration of  
186 the material properties and (2) decrease in the effectively insulated area. On the one hand, the thermal properties may  
187 deteriorate owing to exposure to the environment. On the other hand, insulation boards are likely to lose effects, such  
188 as bulges, damage, or falls, because they are fixed on the surface of buildings by mechanical fixings or adhesives.  
189 Therefore, these factors lead to differences between the actual performance and design values and introduce uncer-  
190 tainty in the building envelope thermal performance. The following paragraphs introduce these two physical factors  
191 and their corresponding mathematical models.

192 *Deterioration of the material properties.* Several researchers have been concerned with the deterioration of insulation  
 193 materials over a long lifetime. In long-term physical and chemical changes, the gas composition of the foam changes  
 194 with time. Diffusion causes a slow change in the U-value of the insulation materials and always takes several years  
 195 or even centuries, until the gas concentration is in equilibrium [34]. Meanwhile, building envelopes may encounter  
 196 severe natural climate conditions such as large temperature differences between indoor and outdoor environments,  
 197 rain, freezing, and thawing [38]. These processes cause problems such as mold growth, weathering, or moisture,  
 198 which lead to the attenuation of material properties. However, it is difficult to quantify the process of aging owing to  
 199 complicated factors and slow process. Current common methods for testing long-term thermal resistance are mainly  
 200 based on accelerating the aging process by exacerbating the exposure conditions[33], slicing, and scaling[49]. Some  
 201 studies have measured the thermal resistance over the years. The measured data of polyisocyanurate boards have been  
 202 gathered since 2002, and the long-term aging model was calculated by Agesim software in [34]. The tested aging  
 203 curve was used to describe the deterioration in the properties of the insulation materials in this study.

204 *Decrease of the effectively insulated area.* A decrease in the effectively insulated area has a negative impact on the  
 205 overall thermal performance of the building envelope. Bulge, damage, and falls are common problems of insulation  
 206 boards in the operation stage of a building, leading to a decrease in the effectively insulated area. The decrease in the  
 207 effect of the insulated area results from many factors, such as the deformation of materials under stress, weak fixation  
 208 by mechanical fixings or adhesives, and extreme weather. When a part of the building envelope uninsulated, the local  
 209 heat loss increases. Therefore, the proportion of uninsulated area to the total area of the building envelope (UAR,  
 210 uninsulated area ratio) was used to quantify the decrease in the effectively insulated area. See Eqs. (1), where  $A_{\text{uninsu}}$   
 211 is the uninsulated area of the external wall (or roof) and  $A_{\text{tot}}$  is the total area of the external wall (or roof). In the next  
 212 section, the mathematical models of physical factors  $AF$  and  $UAR$  are introduced.

$$UAR = \frac{A_{\text{uninsu}}}{A_{\text{tot}}} \quad (1)$$

### 2.1.2. Mathematical models of AF and UAR

213 The relationship between AF and building age is shown in Fig.3 (a). For aged materials, the thermal conductivity  
 214 ( $R$ -value,  $\lambda$ ) becomes the original value multiplied by the aging factor associated with building age. See Eqs. (2),  
 215 where  $t$  is the age of the insulation boards,  $\lambda(t)$  is the thermal conductivity at age  $t$ , and  $AF(t)$  is the aging factor  
 216 at age  $t$ . In general, as the insulation material ages, the thermal performance worsens, which is known from the  
 217 monotonically increasing aging curve, and the aging factor is always greater than 1. The rate of the aging process  
 218 slowed, and the thermal conductivity tended to be stable.

$$\lambda(t) = AF(t) \cdot \lambda(0) \quad (2)$$

220  $UAR$  was assumed to be a time-variant Weibull variable. The Weibull model can reasonably describe the degrada-  
 221 tion and failure processes of both mechanical and electronic components arising from processes such as wear, fatigue,

corrosion, or mechanical overload [50]. In practice, it is widely used in the failure analysis of facilities, such as pipelines [51] and building components [52]. Failure of the fixation of the insulation is considered to be a cumulative process due to wear and tear, which is appropriately described by Weibull function. The mathematical form of the 2-parameter Weibull cumulative distribution function (CDF) is given by Eqs. (3), where  $t$  is the age of the insulation boards,  $UAR(t)$  is the proportion of the failed insulation area of age ( $t$ ),  $m$  is the shape parameter, and  $\eta$  is the scale parameter.

$$UAR(t; m, \eta) = 1 - \exp\left[-\left(\frac{t}{\eta}\right)^m\right] \quad (3)$$

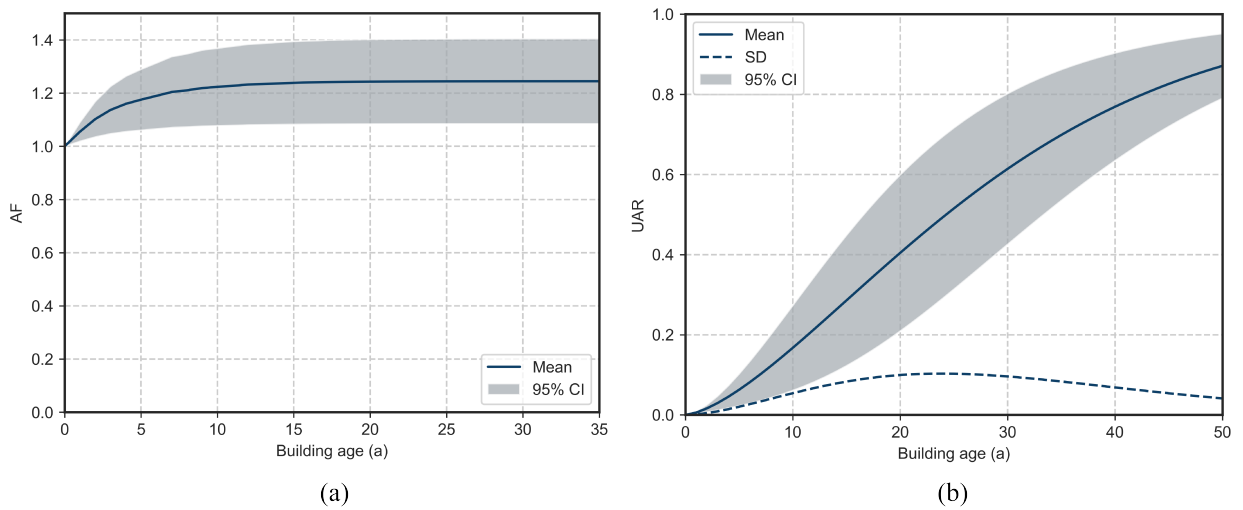


Figure 3: The relationships between physical factors and building age.  $AF$  is used to describe deterioration of the material properties (a), and Average values and  $UAR$  is used to quantify the decrease of the effectively insulated area (b). 95% confidence regions of  $AF$  and  $UAR$  and the standard deviation of  $UAR$  are shown.

However, the  $UAR$  of each building is difficult to accurately quantify. The parameters of the current mathematical model of  $UAR$  were determined based on empirical estimates. The model is regarded as a demo to reflect the failure features to satisfy the need to reveal the impact of uncertainty in U-values on urban-scale heating/cooling demand. Based on empirical estimates of the current state of building stock in China, the shape parameter is taken as 1.5, and the scale parameter is 31. The solid line in Fig.3 (b) shows the relationship between mean  $UAR$  and building age. In China, the current building life expectancy is 50 years and the life expectancy of the insulation system is 25 years. As the model shows,  $UAR$  is 0.5, in year 25, which means almost half of the insulated area would fail. In year 50, the mean  $UAR$  was 0.9, indicating that the building's insulation system would be almost ineffective. In the next section, different thermal transmittance models are introduced.

237    2.1.3. Models of building envelope thermal transmittance

238    The physics-based models of building envelope thermal transmittance generate U-values for UBEM simulation  
239    based on the year built for each building. First, the initial U-value of each building is determined according to the  
240    constraint value in the design standard of the corresponding period. Second, *AF* and *UAR* are obtained according to  
241    building age, based on which the U-value considering aging is calculated. Three models of building envelope thermal  
242    transmittance are compared in this research: base-uniform, aged-uniform, and aged-diverse, as shown in Fig.2.

243    The base-uniform model represents the status-quo approach for UBEM characterization. In building characteri-  
244    zation in traditional UBEMs, the thermal transmittance of the external wall and roof of each building is assumed to  
245    be the constraint value of the design standard corresponding to the year built. In the base-uniform model, buildings  
246    built in the same period will have identical thermal transmittance, which may be inconsistent with our intuition for  
247    the urban building stock, including various buildings. This approach is chosen as the baseline for this research, and  
248    the simulation results of the other two models are compared.

249    In the aged-uniform model, to describe the changes in building envelope thermal transmittance with time, the  
250    discrepancy corresponding to building age between the average U-value and the initial U-value is considered. The  
251    *AF* and *UAR* values of each building are generated based on the building age. Only the mean values of *AF* and  
252    *UAR* are used in this model. Buildings of the same age have the same *AF* and *UAR* and therefore have the same  
253    U-value. Therefore, in the aged-uniform model, the U-values of buildings built in the same period are diversified into  
254    several different values, which are identical to those in the base-uniform model. Buildings built in different years are  
255    of different U-values, and the U-values of the buildings built in the same year are still identical. The aged-uniform  
256    model only considers the discrepancy between the actual U-value and the initial U-value for buildings following the  
257    same standard owing to different building ages.

258    The aged-diversity model further considers stochasticity in the U-value of buildings built in the same year, based  
259    on the aged-uniform approach. Different levels of maintenance and the local environment can lead to uncertainty in  
260    the rate of material deterioration and a decrease in the insulated area of buildings, which both base-uniform and aged-  
261    uniform approaches neglect. To quantify the stochasticity, *AF* and *UAR* of each building are assumed to be normal  
262    variables, and the mean values of *AF* and *UAR* are the same as those in the aged-uniform. Because the deterioration  
263    of the insulation material is irreversible, *AF* in any year is always above 1. Therefore, the distribution form of *AF*  
264    is assumed in Eqs. (4): The lower bound of the  $3\sigma$  interval is equal to 1, and the standard deviation increases with  
265    increasing *AF*, which is consistent with our intuition. The 95% confidence region for *AF* is shown in Fig.3 (a).

$$AF_{sto} \sim N\left(AF_{uni}, \frac{AF_{uni} - 1}{3}\right) \quad (4)$$

266    The standard deviation (SD) of *UAR* is indicated by the dashed line and the 95% confidence region is indicated  
267    by the shaded area in Fig.3 (b). In the early stage of building construction, buildings of the same age are in good  
268    condition, and the deviation in *UAR* is small. For buildings that have been built for 20 to 30 years (insulation system

269 life expectancy), building performance varies widely: some buildings are still well insulated, whereas the insulation  
 270 systems of some buildings are almost invalid. However, the deviation of *UAR* decreases for buildings with older age  
 271 because the majority of buildings would be poorly insulated after a long period of service. Compared with the constant  
 272 SD, the time-variant SD of *UAR* distribution provides a better depiction of the stochasticity of the U-values. Therefore,  
 273 in the aged-diverse approach, buildings built in different years are of different thermal performance affected by aging,  
 274 and the buildings built in the same year are also diversified. The stochasticity is propagated from the probabilistic  
 275 distributions of *AF* and *UAR* to U-values.

276 Both aged-uniform and aged-diverse models consider changes in the thermal performance from the design. The  
 277 impacts of material deterioration and the decrease in the effectively insulated area are depicted by *AF* and *UAR* based  
 278 on the thermal resistance of the insulation board and solid wall or slab. In the design stage, the thermal resistance  
 279 of the building envelope can be decomposed into four parts: convective thermal resistance of the inner surface  $R_{in}$ ,  
 280 convective thermal resistance of the outer surface  $R_{out}$ , conductive thermal resistance of the insulation board  $R_{insu}$  and  
 281 conductive thermal resistance of the solid wall or slab  $R_{base}$ . See Eqs. (5). Because the U-values of the insulated and  
 282 uninsulated areas are different, the U-value generated by the aged approaches is the average of the insulated U-value  
 283 and the uninsulated U-value weighted by the area proportions [44] according to Eqs. (6). The differences in fidelity  
 284 among the three approaches are summarized in Table 1.

$$U_{base} = \frac{1}{R_{design}} = \frac{1}{R_{in} + R_{out} + R_{insu} + R_{base}} \quad (5)$$

$$U_{aged} = \frac{1}{R_{aged}} = \frac{1 - UAR}{R_{in} + R_{out} + R_{insu}/AF + R_{base}} + \frac{UAR}{R_{in} + R_{out} + R_{base}} \quad (6)$$

Table 1: Differences in fidelity among the three approaches.

| Approach     | Fidelity                      | Description   |
|--------------|-------------------------------|---|
| Base-uniform | No uncertainty                | U-values are assumed identical with constraint U-values in design standards.  |
| Aged-uniform | Discrepancy                   | Changes in average U-values with time are considered through <i>AF</i> and <i>UAR</i> correspond to building age.               |
| Aged-diverse | Discrepancy and stochasticity | Stochasticity in U-values among buildings of the same age is considered through the distributions of <i>AF</i> and <i>UAR</i> . |

## 285 2.2. Urban building energy modeling

286 DeST-urban, a platform for urban building energy modeling, was developed and used for the UBEM simulation  
 287 in this research. DeST-urban uses a physics-based, bottom-up approach for urban building energy modeling. Each  
 288 building in the stock is modeled using its real location and geometric information, with typical building characteristics  
 289 determined by the building usage. Physics-based building energy models (BEMs) are automatically generated and  
 290 simulated in parallel by multiprocessor servers [53]. The building energy simulation engine is DeST, a whole-building

291 energy modeling program developed by Tsinghua University, China [54, 55] and is based on a state-space multi-zone  
 292 heat balance calculation method [56, 57]. The input of DeST-urban is the CityGML 3D city model [58], which is  
 293 widely used in urban energy simulations [59], including the building footprint, height, number of layers, usage type,  
 294 and year built. The outputs were the hourly heating and cooling demands of each building.

295 The usage of lighting, plugs, HVAC, and occupant schedules are configured according to prototype building  
 296 models for each building usage based on actual energy consumption[60]. The simulations used typical meteorological  
 297 year (TMY) data for Beijing, generated from 10 weather stations. The location of the weather stations are shown in  
 298 Fig.5. The weather station with the shortest linear distance provided weather data for each building to ensure that each  
 299 BEM was based on the local climate.

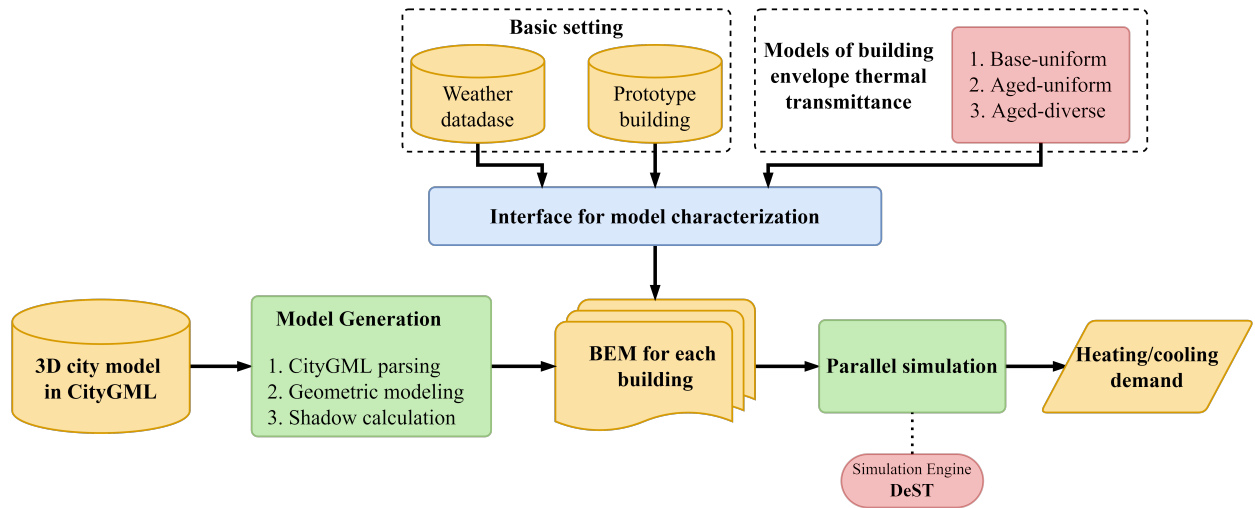


Figure 4: Simulation framework of DeST-urban with models of building envelope thermal transmittance.

300 The simulation framework of DeST-urban with the integrated building envelope thermal transmittance models  
 301 is shown in Fig.4. The 3D city model was parsed by the platform, and the basic information of each building was  
 302 extracted for model generation. Subsequently, a geometric model of each building was established, and the shadow  
 303 interaction in the neighborhood was calculated using the DeST-urban platform. After the shadow calculation, solar  
 304 heat gain of each building could be calculated using the sunlit areas of the building surfaces. BEM of each building is  
 305 generated and stored in the form of a database so that the attributes of the BEM can be set via the pre-defined standard  
 306 interface. The basic characteristics of BEMs are set according to databases of weather and prototype buildings, such  
 307 as weather conditions, occupancy, equipment, and lighting usage. Distributions of the building envelope thermal  
 308 transmittance can be generated and passed to the BEMs via the standard interface.

309 In this study, three physics-based models of building envelope thermal transmittance generated different distribu-  
 310 tions of the U-value of the building stock. UBEM was characterized based on the three models of building envelope  
 311 thermal transmittance proposed in Section 2.1.3. In the base-uniform approach, U-values of the external walls and

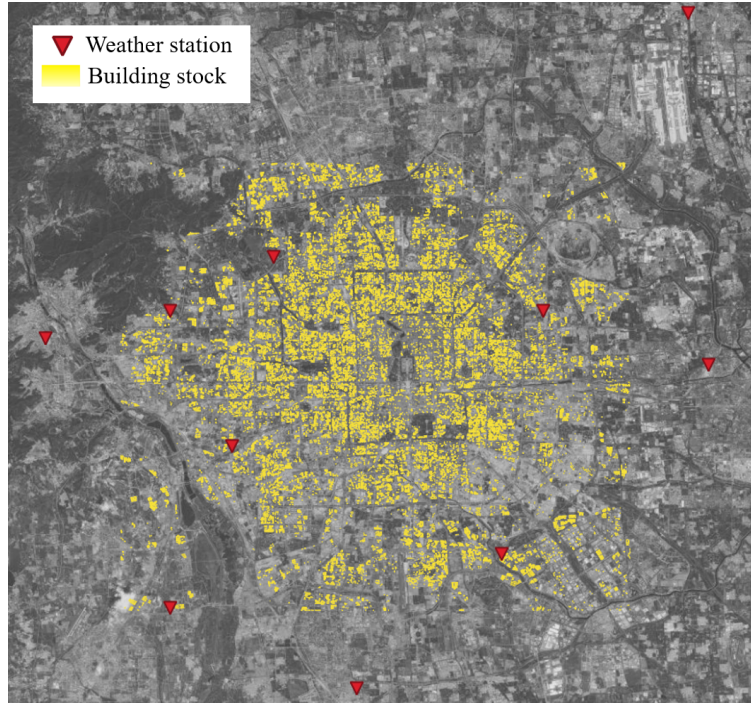


Figure 5: Spatial distribution of the building stock and weather stations in case study

312 roof of each building were consistent with design standards. U-values specified in each standard represented the  
 313 building envelope thermal performance of a group of buildings built in the period of validity. In the aged-uniform  
 314 approach, time-related discrepancy in U-values was further considered based on the identical design U-values of a  
 315 group of buildings in the base-uniform approach. Specifically, *AF* and *UAR* were used to modify the U-value accord-  
 316 ing to the building age. While in the aged-diverse approach, stochasticity in U-values among buildings built in the  
 317 same year was considered and the distribution of *AF* and *UAR* was used to generate the distribution of U-values by  
 318 Monte Carlo method. The hourly heating and cooling demand of each building was calculated using the platform. In  
 319 the subsequent processing, heating/cooling demands were aggregated by different temporal and spatial resolutions for  
 320 analysis.

### 321 2.3. Comparison method

322 To answer research questions (Q2) and (Q3), the heating/cooling demand of building stock calculated by the three  
 323 different approaches were compared in the different dimensions of time and space as well as for different application  
 324 scenarios.

325 The hourly and diurnal profiles of the heating/cooling demand were analyzed to understand the impact of uncer-  
 326 tainty on temporal patterns. In addition, the annual total heating/cooling demand at the urban scale was chosen as  
 327 a metric because of its breadth of application in district thermal load simulations. The hourly, diurnal, and annual  
 328 heating/cooling demands at the urban scale were aggregated by the hourly heating/cooling demand of each building.

329 See Eqs. (7) and (8), where  $h_k^i(j)$  is the heating demand of building  $k$  at hour  $i$  on day  $j$ ;  $c_k^i(j)$  is the cooling demand  
 330 of building  $k$  at hour  $i$  on day  $j$ ;  $H_{\text{hour}}^i(j)$  is the heating demand at urban scale at hour  $j$  on day  $i$ ;  $C_{\text{hour}}^i(j)$  is the cooling  
 331 demand at urban scale at hour  $j$  on day  $i$ ;  $H_{\text{di}}^i$  is the diurnal heating demand on day  $i$  at urban scale;  $C_{\text{di}}^i$  is the diurnal  
 332 cooling demand on day  $i$  at urban scale;  $H_{\text{ann}}$  is the annual heating demand at urban scale;  $C_{\text{ann}}$  is the annual cooling  
 333 demand at urban scale; and  $N$  is the total number of buildings.

$$H_{\text{ann}} = \sum_{i=1}^{365} H_{\text{di}}^i = \sum_{i=1}^{365} \sum_{j=1}^{24} H_{\text{hour}}^i(j) = \sum_{i=1}^{365} \sum_{j=1}^{24} \sum_{k=1}^N h_k^i(j) \quad (7)$$

$$C_{\text{ann}} = \sum_{i=1}^{365} C_{\text{di}}^i = \sum_{i=1}^{365} \sum_{j=1}^{24} C_{\text{hour}}^i(j) = \sum_{i=1}^{365} \sum_{j=1}^{24} \sum_{k=1}^N c_k^i(j) \quad (8)$$

334 The diversity of heating/cooling demands of individual buildings has attracted increasing concern because of its  
 335 great impact on policy and the deployment of technology. The annual heating/cooling demand per unit floor area  
 336 of each building was calculated to indicate the demand intensity, as shown in Eqs. (9) and (10), where  $HI_k$  is the  
 337 annual heating intensity of building  $k$ ,  $CI_k$  is the annual cooling intensity of building  $k$ , and  $A_k$  is the total floor area  
 338 of building  $k$ :

$$HI_k = \frac{\sum_{i=1}^{365} \sum_{j=1}^{24} h_k^i(j)}{A_k} \quad (9)$$

$$CI_k = \frac{\sum_{i=1}^{365} \sum_{j=1}^{24} c_k^i(j)}{A_k} \quad (10)$$

339 The demand intensity distributions of the building stock were analyzed to investigate the impact of uncertainty in  
 340 building envelopes on the population characteristics of building heating/cooling demand. The relationships between  
 341 the distributions of heating demand intensity and building age were analyzed to explore the fidelity of the different  
 342 approaches. In addition, the aged-uniform and aged-diverse approaches are further compared on the deviation of  
 343 heating demand intensity of buildings at different levels of demand to understand the impact of discrepancy and  
 344 stochasticity in building envelope thermal transmittance.

### 345 3. Case study

346 A residential building stock in Beijing containing 33,222 buildings was used as a case study to analyze the impact  
 347 of building envelope thermal transmittance on urban heating and cooling demand. The building footprint and number  
 348 of stories for each building were obtained as shown in Fig.5. The floor area of the building stock is 3.4 million m<sup>2</sup>  
 349 and follows a right-skewed distribution with a median floor area of 7,650m<sup>2</sup>, as shown in Fig.6(a). The geometry  
 350 was simplified as 2.5D building blocks by removing details such as the tilted roof and setbacks with increasing tower

height. The height of the building was generated according to a floor-to-floor height of 2.85m and the overall window-to-wall ratio was 0.26 for each building, according to a prototype building model based on actual energy consumption [60]. More details on UBEM characterization are provided in Appendix A.

The year built for each building was not provided in this case, although the data could be more accessible as studies on urban building stock became more important. In addition, the aim of this research is to quantify the impact of the uncertainty of building envelope thermal transmittance on urban heating/cooling demand, which indicates that a high-fidelity distribution of building age is sufficient for subsequent analysis, although it is not necessary to clarify the exact year built for each building.

Therefore, the distribution of the buildings' year of construction was estimated according to the floor space completed each year in the latest statistical yearbook of Beijing. The proportion of the completed area each year represents the proportion of buildings built in each year in the entire building stock. The year built for each building was sampled from the probability distribution in data pre-processing. Buildings built after 1987 were considered when China's first building energy-efficiency design standard was implemented. Buildings built before 1987 accounted for a small proportion of existing residential buildings in Beijing, and most of them were installed with insulation systems after 1987. Buildings built before 2018 were considered, as the information in the 3D city model was collected in 2018. Fig.6(b) shows the number of buildings built in each year. The number of buildings completed each year increased in the 1990s, peaking at the beginning of the century, and gradually decreasing thereafter.

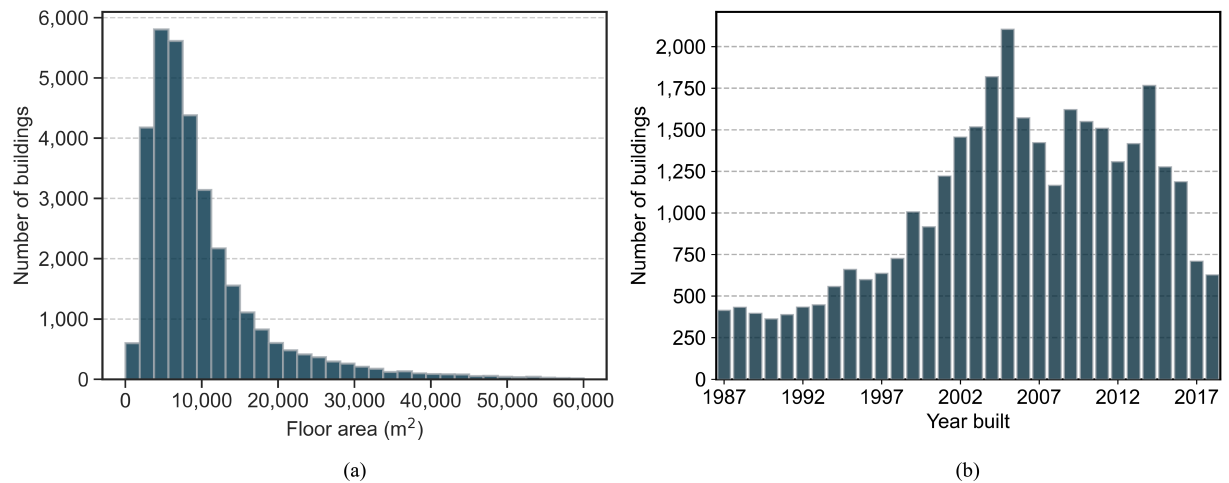


Figure 6: The distribution of floor area (a) and year built (b) of the building stock.

#### 4. Results

Three physics-based models of building envelope thermal transmittance were compared in the building stock, considering the discrepancy between the average U-values and the initial U-values and the stochasticity among different

371 buildings. In this section, the distributions of thermal transmittance generated by different approaches are presented.  
 372 The aggregated heating/cooling demands are then shown, including the hourly and diurnal profiles and annual total  
 373 demand. Finally, the heating/cooling demand distributions of each building were analyzed.

374 *4.1. Envelope thermal transmittance*

375 Beijing is part of the cold region in China with a long heating period. Based on the standards for cold regions[61,  
 376 62, 63], building envelopes are divided into three categories according to the differences in the construction periods,  
 377 as shown in Table 2. In the base-uniform approach, constraint values in standards are used to represent in-situ thermal  
 378 transmittance; therefore, the U-values in each standard are mapped to all buildings built in the implementation period  
 379 of the standard. In the aged-uniform approach, the aging processes in the insulation of the external wall and roof were  
 380 considered. The discrepancy between the average U-values and initial U-values is described, and the discrepancy  
 381 varies with building age. In the aged-diverse approach, the stochasticity among buildings built in the same year was  
 382 also considered, and the actual distributions of U-values were generated based on the normal distribution assumptions  
 383 of the physical factors.

Table 2: Initial values of building envelope thermal performance in different construction periods.

| Parameters                                | 1987-1995[61] | 1996-2010[62] | 2011-2018[63] |
|---|---------------|---------------|---------------|
| Wall U-value [W/(m <sup>2</sup> · K)]     | 1.60          | 0.83          | 0.70          |
| Roof U-value [W/(m <sup>2</sup> · K)]     | 0.91          | 0.60          | 0.45          |
| Window U-value [W/(m <sup>2</sup> · K)]   | 6.40          | 4.70          | 2.50          |
| Window solar heat gain coefficient (SHGC) | 0.39          | 0.39          | 0.39          |

384 Fig.7 shows the U-values of external wall and roof generated by three different models. In the base-uniform ap-  
 385 proach, with only the initial U-values considered, the U-values of the external wall are concentrated in three constraint  
 386 values in the corresponding standards, and the phenomenon of the roof is similar. Considering the discrepancy be-  
 387 tween the U-values and initial U-values of the buildings following the same standards, the U-values of the building  
 388 stock are broken down into several values relevant to the building age in the aged-uniform approach. However, the  
 389 U-values are still a series of discrete values, not a continuous distribution, which remains a gap from the real situation  
 390 of the U-values of urban buildings. In the aged-diverse approach, the stochasticity in the U-values of buildings built  
 391 in the same year is considered in continuous distributions. The diversified, continuous distributions are closer to the  
 392 reality of the thermal transmittance of the building envelope in the building stock. Table.3 and 4 give descriptive  
 393 statistics for U-values in aged-uniform and aged-diverse approaches. Comparing the statistics of U-values in each  
 394 vintage, it is found that the relationship between the aging effect and building vintage is reflected in the two aged  
 395 approaches. For buildings built between 2011 and 2018, the lower bounds of the U-value distributions are quite close  
 396 to the constraint values, as some buildings have just been built and the building envelopes are in good condition.  
 397 However, the envelopes of the buildings built before had worse thermal performance relative to the initial U-values.

398 Comparing the U-values generated by the two approaches, the U-values in the aged-diverse approach have a larger  
 399 dispersion than those in the aged-uniform approach. Considering the stochasticity in the U-values of buildings built  
 400 in the same year further diversifies the U-values of the building stock.

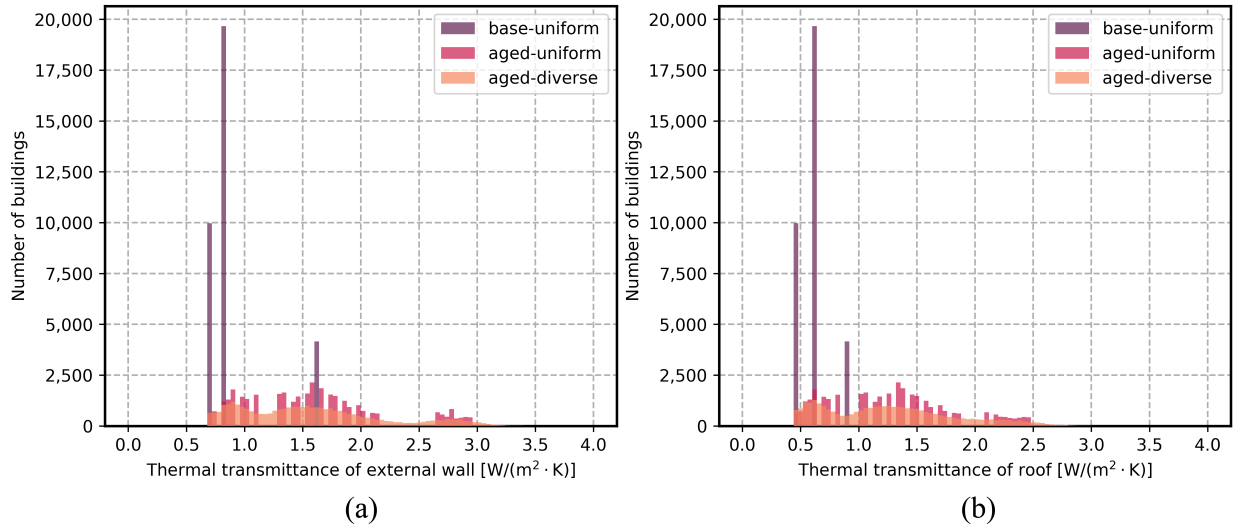


Figure 7: U-values of external wall (a) and roof (b) generated by three different models.

Table 3: Statistical summary of U-values of external wall [W/(m<sup>2</sup>·K)] by building vintages in aged-uniform and aged-diverse approaches. The values in parentheses are the initial U-values in design, used in base-uniform approach.

| Building vintage | 1987-1995 (1.60) |              | 1996-2010 (0.83) |              | 2011-2018 (0.70) |              | All          |              |
|------------------|------------------|--------------|------------------|--------------|------------------|--------------|--------------|--------------|
| Method           | aged-uniform     | aged-diverse | aged-uniform     | aged-diverse | aged-uniform     | aged-diverse | aged-uniform | aged-diverse |
| 2%               | 2.65             | 2.36         | 1.28             | 1.13         | 0.70             | 0.70         | 0.75         | 0.73         |
| 25%              | 2.69             | 2.64         | 1.47             | 1.41         | 0.80             | 0.82         | 1.09         | 1.06         |
| 50%              | 2.76             | 2.79         | 1.66             | 1.63         | 0.91             | 0.91         | 1.53         | 1.50         |
| 75%              | 2.87             | 2.94         | 1.85             | 1.88         | 1.03             | 1.01         | 1.85         | 1.92         |
| 98%              | 2.94             | 3.21         | 2.16             | 2.37         | 1.09             | 1.21         | 2.90         | 2.99         |

Table 4: Statistical summary of U-values of roof [W/(m<sup>2</sup>·K)] by building vintages in aged-uniform and aged-diverse approaches. The values in parentheses are the initial U-values in design, used in base-uniform approach.

| Building vintage | 1987-1995 (0.91) |              | 1996-2010 (0.60) |              | 2011-2018 (0.45) |              | All          |              |
|------------------|------------------|--------------|------------------|--------------|------------------|--------------|--------------|--------------|
| Method           | aged-uniform     | aged-diverse | aged-uniform     | aged-diverse | aged-uniform     | aged-diverse | aged-uniform | aged-diverse |
| 2%               | 2.11             | 1.77         | 1.02             | 0.86         | 0.45             | 0.45         | 0.49         | 0.48         |
| 25%              | 2.16             | 2.10         | 1.20             | 1.14         | 0.53             | 0.55         | 0.81         | 0.78         |
| 50%              | 2.26             | 2.29         | 1.39             | 1.35         | 0.64             | 0.63         | 1.26         | 1.23         |
| 75%              | 2.39             | 2.47         | 1.57             | 1.60         | 0.75             | 0.73         | 1.57         | 1.63         |
| 98%              | 2.47             | 2.80         | 1.87             | 2.08         | 0.81             | 0.92         | 2.43         | 2.54         |

401 4.2. Aggregated heating/cooling demand at urban scale

402 4.2.1. Hourly and diurnal profiles

403 Fig.8 shows the simulated results of heating and cooling demand. Hourly profiles on typical days and diurnal  
404 profiles of the year are presented. The diurnal heating demand at urban scale  $H_{di}$  is shown in Fig.8(a), the hourly  
405 heating demand  $H_{hour}$  from January 4th to January 7th is shown in Fig.8(b), (c) shows diurnal cooling demand  $C_{di}$  and  
406 (d) shows the hourly cooling demand  $C_{hour}$  from July 19th to July 22nd. 10 repeated simulation results in aged-diverse  
407 approach are all shown in Fig.8, while the profiles overlap, which is discussed in Section 5.

408 The differences in the curves among the three approaches in each figure are a result of the uncertainty of the  
409 building envelope thermal transmittance, including both the discrepancy and stochasticity; the rest of the building  
410 model characteristics remain equal. As shown in Fig. 8, the curves in aged approaches considering uncertainty are  
411 quite different from that neglecting uncertainty. Considering the uncertainty in thermal transmittance, the profiles of  
412 the heating and cooling demand are always above the profile, neglecting the uncertainty in the base-uniform approach.  
413 However, the curves in the aged approaches are almost identical, which means that the discrepancy between the  
414 average U-values and the initial U-values must be considered in terms of diurnal or hourly profiles, whereas the  
415 stochasticity in U-values among the buildings built in the same year could be neglected.

416 As shown in Fig.8(b) and (d), the simulated hourly profiles of  $H_{hour}$  and  $C_{hour}$  generated by three approaches are  
417 similar in shape, since changes in thermal transmittance of building envelopes will not result in changes in phase  
418 position of load profiles and the continuous impact of changes has little effect on the time-series characteristic of  
419 profiles. However, the magnitudes of the impact are different for  $H_{hour}$  and  $C_{hour}$ :  $H_{hour}$  considering the uncertainty of  
420 thermal transmittance is consistently greater than that in the base-uniform approach, whereas the differences in  $C_{hour}$   
421 are smaller between the aged and base-uniform approaches, which means that the uncertainty of thermal transmittance  
422 has a greater impact on  $H_{hour}$  than  $C_{hour}$ . In addition, as shown in Fig.8(a), the differences between the profile of  $H_{di}$   
423 considering uncertainty and that neglecting uncertainty are greater when the  $H_{di}$  is higher, especially on extremely  
424 cold days, since the deterioration in the overall performance of building envelopes leads to more heat loss when  
425 indoor and outdoor temperature difference is high.

426 4.2.2. Annual total heating/cooling demand at urban scale

427 The total annual heating/cooling demand at the urban scale ( $H_{ann}/C_{ann}$ ) is shown in Fig.9.  $H_{ann}/C_{ann}$  in the base-  
428 uniform and aged-uniform approaches are point values, while in the aged-diverse approach,  $H_{ann}/C_{ann}$  in 10 repeated  
429 simulations are shown in the boxplots in Fig.9. The stability of different simulation results is discussed in Section  
430 5. After considering the uncertainty of the building envelope thermal transmittance,  $H_{ann}$  increases because the de-  
431 terioration trend of the insulation system leads to an increase in heat loss during the heating period. A similar trend  
432 is found in  $C_{ann}$  because the room temperature is higher when considering the aging effect of the building envelope,  
433 which increases the cooling demand when people are at home.  $H_{ann}/C_{ann}$  and the change percentages after considering  
434 the uncertainty in the thermal transmittance are listed in Table.5. Considering the uncertainty in the building envelope

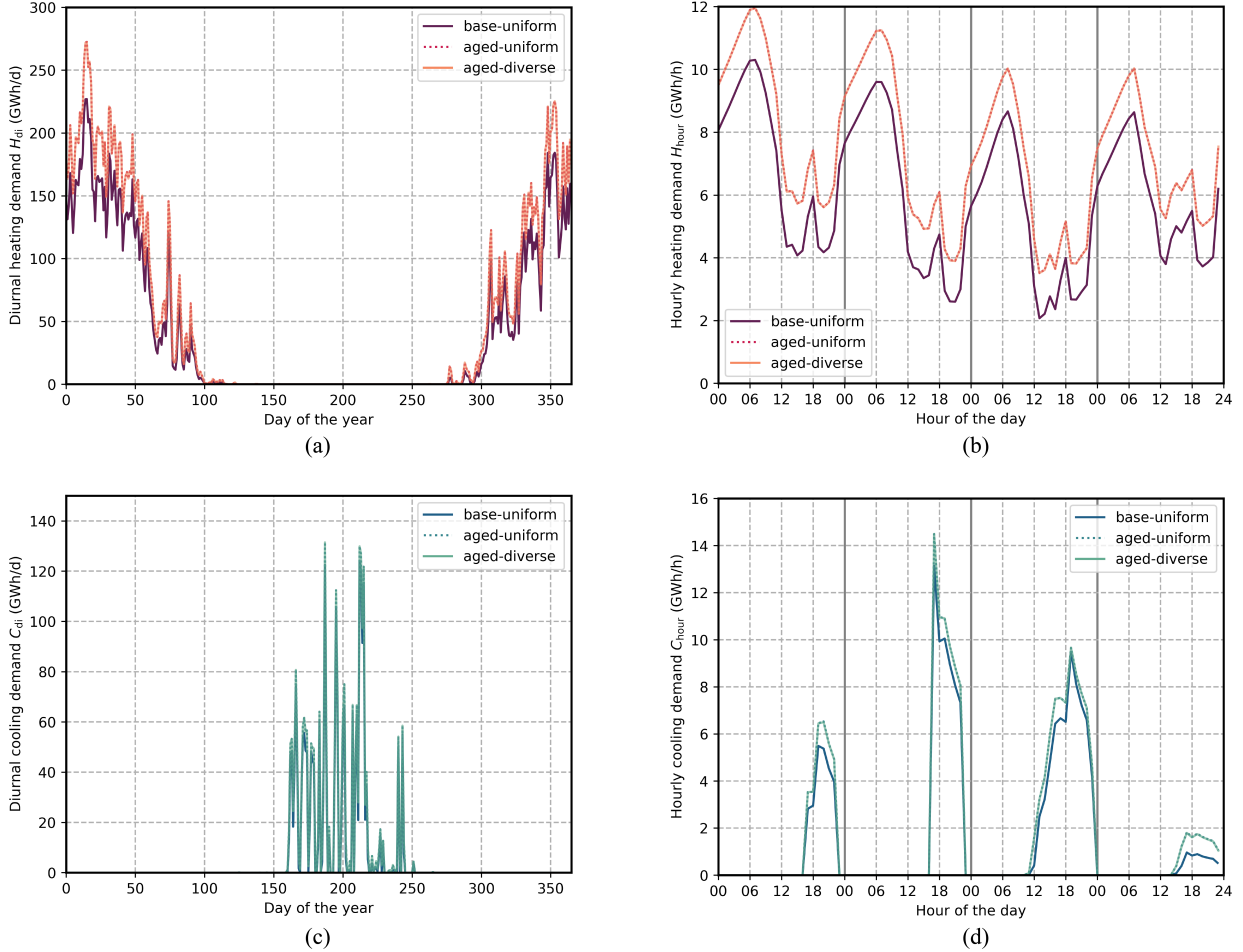


Figure 8: Comparison of simulated heating and cooling demand by the three approaches. Subplot (a) shows results for  $H_{di}$  and (b) shows results for  $H_{hour}$ . Subplot (c) shows results for  $C_{di}$  and (d) for  $C_{hour}$  in typical days. 10 repeated simulation results in aged-diverse approach are all shown.

435 thermal transmittance,  $H_{ann}$  increased by 26%, whereas  $C_{ann}$  increased by 13%. The impact of uncertainty on  $H_{ann}$   
 436 was greater than that on  $C_{ann}$ . In addition,  $H_{ann}$  value of the residential building stock in Beijing was much greater than  
 437  $C_{ann}$ . The weather dictates that Beijing's heating demand in winter is greater than its cooling demand in summer. On  
 438 the other hand, split air conditioners are the main equipment for residential cooling in Beijing, and the air conditioners  
 439 are operated part-time when people are at home. District heating is the main method of residential heating in Beijing,  
 440 and full-time heating was considered in the heating demand simulation.

441 However, for the two possible causes of the diversity of building envelope thermal transmittance, the discrepancy  
 442 in U-values of buildings built in different years has a greater impact on  $H_{ann}$  and  $C_{ann}$  than stochasticity in U-values  
 443 of buildings built in the same year.  $H_{ann}$  in the aged-uniform and aged-diverse approaches were almost identical, and  
 444 the same was observed in  $C_{ann}$ . For buildings built in the same year, the U-values obtained using the aged-uniform  
 445 approach were identical, and the U-values were regarded as the mean values of the U-value distributions obtained

446 using the aged-diverse approach. Therefore, the total demand is almost identical in the aged approach when all  
447 buildings are aggregated.

Table 5: Annual total heating and cooling demand ( $H_{\text{ann}}$  and  $C_{\text{ann}}$ ).  $H_{\text{ann}}/C_{\text{ann}}$  in the aged-diverse approach is the average of 10 repeated simulations. The values in parentheses are normalized to the results of base-uniform approach.

| Method       | $H_{\text{ann}}$ (TWh/a) | $C_{\text{ann}}$ (TWh/a) |
|--------------|--------------------------|--------------------------|
| base-uniform | 16.57 (1)                | 2.20 (1)                 |
| aged-uniform | 20.85 (1.26)             | 2.48 (1.13)              |
| aged-diverse | 20.84 (1.26)             | 2.48 (1.13)              |

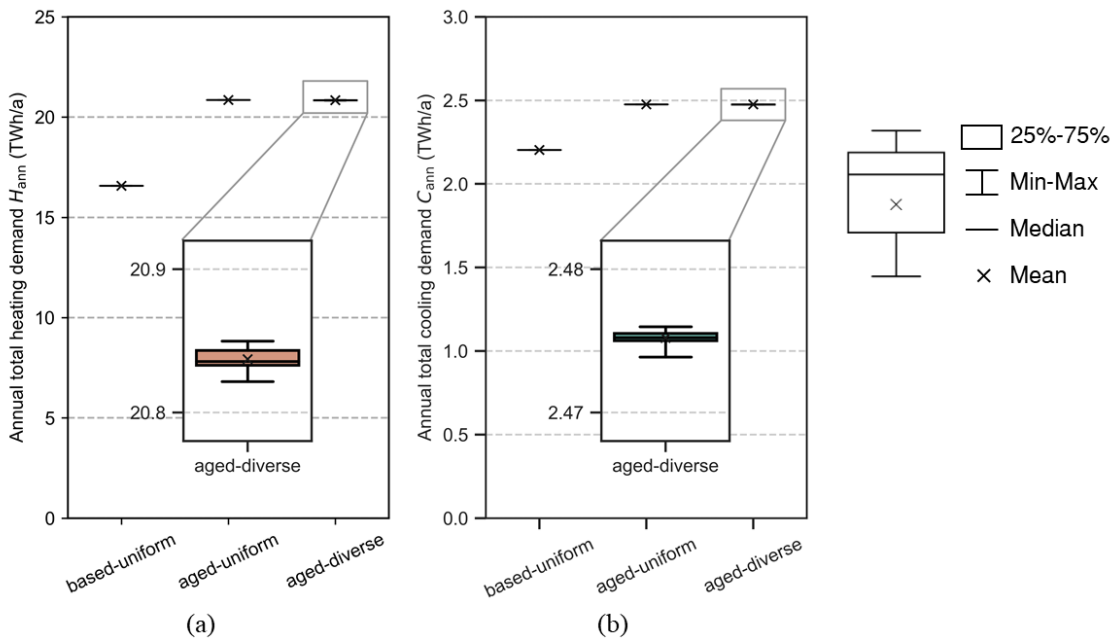


Figure 9: Annual total heating demand  $H_{\text{ann}}$  (a) and cooling demand  $C_{\text{ann}}$  (b) of the building stock in three approaches.

#### 448 4.3. Building heating/cooling demand distribution

449 The distributions of building demand intensity  $HI_k$  and  $CI_k$  are presented in Fig.10. As shown in the figures,  $HI_k$   
450 and  $CI_k$  follow right-skewed distributions. The impact of uncertainty in thermal transmittance on  $HI_k$  distribution is  
451 greater than that on  $CI_k$  distribution. The overall distribution of  $HI_k$  changes in the direction of  $HI_k$ , and the peak of  
452 the histogram drops. For  $CI_k$ , the differences between the distributions of the three approaches are smaller. Table.6  
453 presents the quartiles of the distribution of  $HI_k$  and  $CI_k$ . Considering the discrepancy, the quartiles of the distribution  
454 of  $HI_k$  increase, and the interquartile range also increases, which means that the discrepancy in thermal transmittance  
455 increases the dispersion of the heating demand. The dispersion of the heating demand further increases when consid-  
456 ering both the discrepancy and stochasticity. The interquartile range of the aged-diverse approach increased compared

457 with that of the aged-uniform approach. However, the changes were smaller in the distribution of  $CI_k$  considering the  
 458 uncertainty, since heat transfer through building envelopes has a smaller impact on cooling demand than on heating  
 459 demand. The temperature difference between indoor and outdoor in the cooling period is smaller than that in the  
 460 heating period.

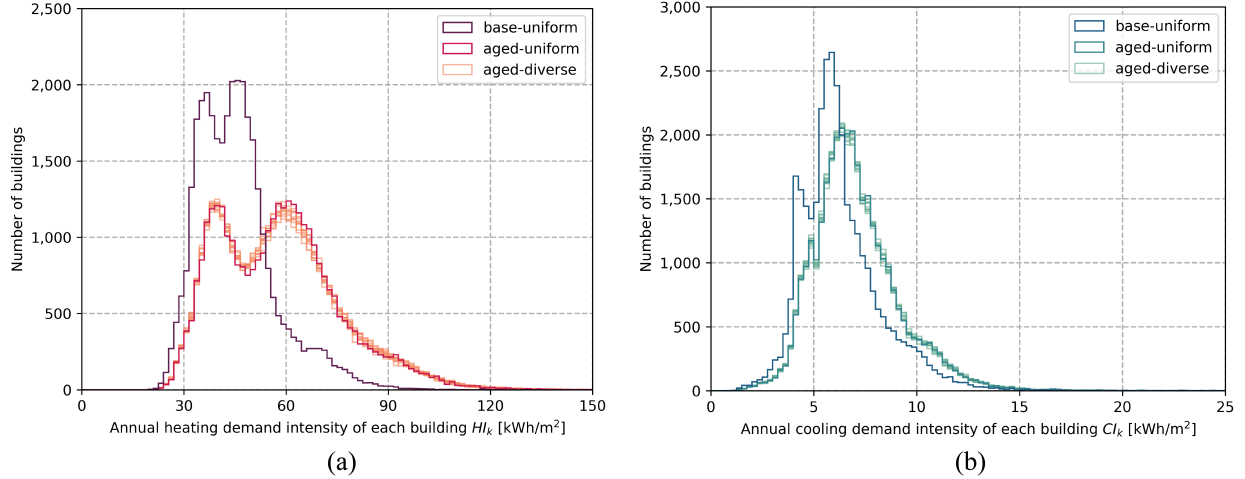


Figure 10: Annual heating/cooling demand intensity ( $HI_k/CI_k$ ) of each building. 10 repeated simulation results of  $HI_k$  and  $CI_k$  distributions in aged-diverse approach are all shown.

Table 6: Statistical summary of  $HI_k$  and  $CI_k$  of each building.

|                             | Heating [ $\text{kWh}/(\text{m}^2 \cdot \text{a})$ ] |              |              | Cooling [ $\text{kWh}/(\text{m}^2 \cdot \text{a})$ ] |              |              |
|-----------------------------|--|--------------|--------------|--|--------------|--------------|
|                             | base-uniform   | aged-uniform | aged-diverse | base-uniform   | aged-uniform | aged-diverse |
| 25% (Q1)                    | 36.89  | 43.21        | 43.01        | 5.04   | 5.72         | 5.71         |
| 50% (Q2)                    | 44.10  | 57.23        | 56.78        | 5.97   | 6.79         | 6.79         |
| 75% (Q3)                    | 50.76  | 68.23        | 68.51        | 7.21   | 8.15         | 8.16         |
| Interquartile Range (Q3-Q1) | 13.87  | 25.02        | 25.5         | 2.17   | 2.43         | 2.45         |

461 The changes in the distributions of  $HI_k$  and  $CI_k$  are smaller considering the stochasticity compared to considering  
 462 only the discrepancy, as shown in Fig.10. Due to the wide range of building age, the aged-uniform approach diversifies  
 463 the U-values from three values to over thirty values, and therefore the improvement in aged-diverse approach is  
 464 limited.

465 Kolmogorov-Smirnov test is conducted to verify whether building heating/cooling demand intensities by different  
 466 approaches have the same continuous distribution. For heating demand, the results indicate the significant differences  
 467 in the distributions of  $HI_k$  by the three approaches. For cooling demand, the distributions by the aged-uniform ap-  
 468 proach and the aged-diverse approach significantly differ from that by the base-uniform approach. However, there are  
 469 no significant differences in the distribution of  $CI_k$  between the aged-uniform approach and the aged-diverse approach,  
 470 since the U-value has a smaller impacts on cooling demand than on heating demand. The results of Kolmogorov-

471 Smirnov test are listed in Appendix B.

472 To understand the impact of stochasticity in buildings built in the same year, 2D histograms of  $HI_k$  and the year  
473 built are presented in Fig.11. The colors indicate the number of buildings with a thermal demand within a specific  
474 range. It can be observed that buildings built in different years have similar distributions if they are characterized  
475 by the same U-values in the base-uniform approach, as shown in Fig.11 (a). In aged-uniform and aged-diverse  
476 approaches that consider uncertainty, the differences among the  $HI_k$  distributions of buildings built in different years  
477 are reflected. As shown in Fig.11 (b) and (c),  $HI_k$  values where the majority of the buildings built in each year are  
478 concentrated decrease with increasing year built.  $HI_k$  values of buildings that follow the same standard are further  
479 diversified than those neglecting uncertainty. Considering stochasticity, the diversity of  $HI_k$  of buildings built in the  
480 same year is enhanced, which can be observed by comparing Fig.11 (b) and (c). Therefore, the stochasticity of the  
481 building influences the  $HI_k$  distribution of buildings built in a particular year. From the analysis of 2D histograms, it  
482 can be found that stochasticity has a greater impact on  $HI_k$  distribution in the energy modeling of building stock with  
483 a smaller range of vintage, as the differences can be seen among the distributions of buildings built in a particular year.  
484 However, the impact of stochasticity is small when the entire building stock with a wide range of vintages is analyzed.

485 To further analyze the heating demand changes considering discrepancy and stochasticity,  $HI_k$  by age approach-  
486 es categorized by levels of heating demand are shown in Fig.12. For better visualization, the results of the three  
487 approaches for each building are categorized and sorted by  $HI_k$  in the base-uniform approach. Therefore, boxes of  
488 the same horizontal coordinate can be used to compare the deviation of  $HI_k$  using an aged-uniform and aged-diverse  
489 approach for the same group of buildings. Considering the physical factors affecting the U-values, the uncertainty of  
490 the building envelope thermal transmittance has a unidirectional impact on  $HI_k$  of each building, causing an increase  
491 in  $HI_k$ . However, the effect of this increase was inconsistent. For buildings with higher  $HI_k$  in the base-uniform  
492 approach,  $HI_k$  increases more after considering uncertainty. Buildings with high  $HI_k$  in the base-uniform approach  
493 indicate an earlier year built. The U-values increase more for buildings with older ages compared to the U-values in  
494 the base-uniform approach because the aging effects on the building envelope are stronger.

495 Fig. 12 shows the impact of stochasticity of U-values on  $HI_k$  more clearly. For a particular level of  $HI_k$  in the base-  
496 uniform approach, the range of  $HI_k$  becomes wider after considering stochasticity compared with that considering  
497 only the discrepancy. Therefore, both the discrepancy and stochasticity of the U-values impact the heating demand  
498 distribution of the building stock.

## 499 5. Discussion

500 In this section, the stability of the multiple simulation results is discussed. The appropriate approach for modeling  
501 the building envelope thermal transmittance for different UBEM simulation purposes and the associated applications  
502 are summarized to answer research question Q3.

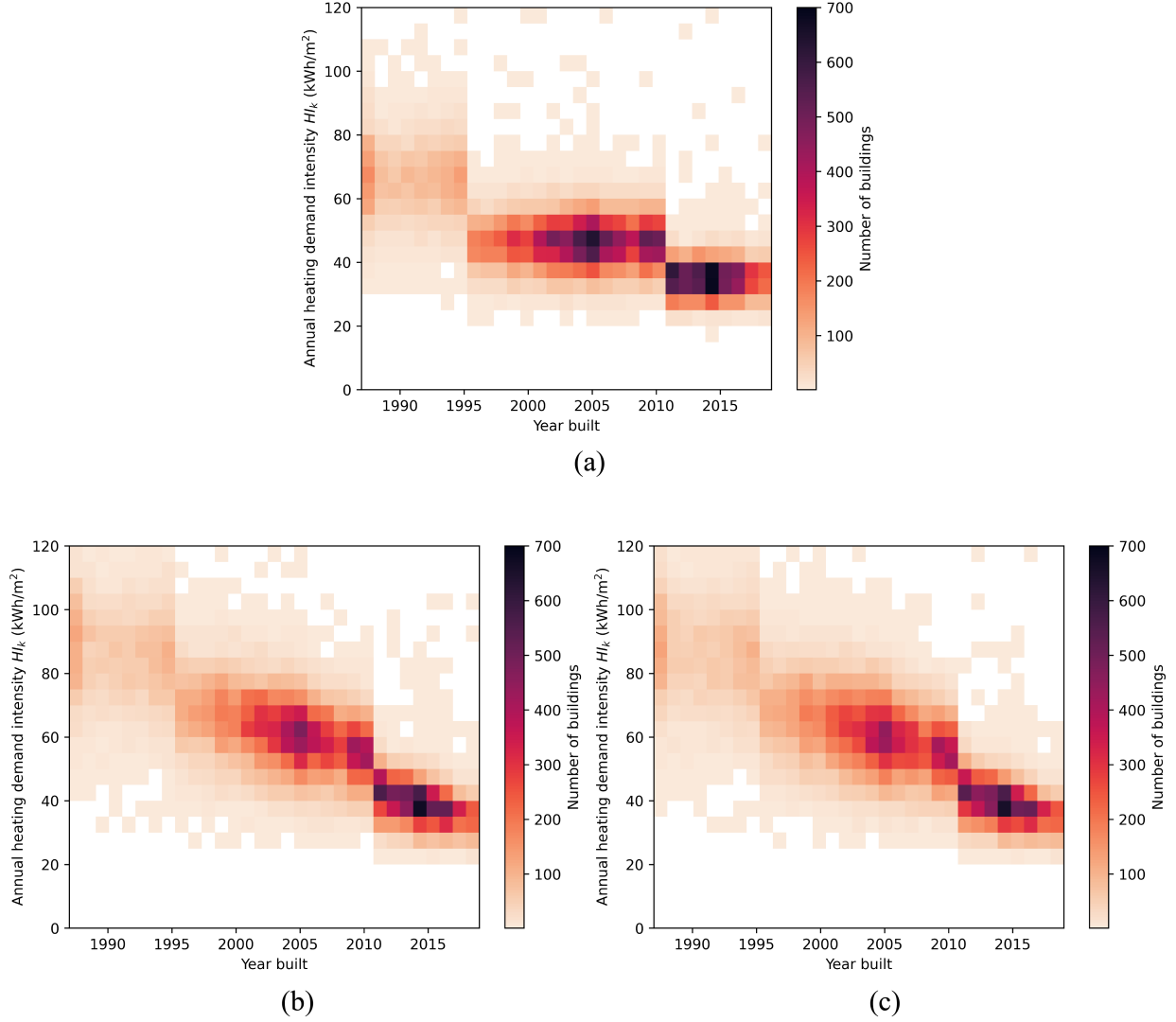


Figure 11: 2D histogram of annual  $HI_k$  vs. year built of each building. Results simulated by base-uniform (a), aged-uniform (b) and aged-diverse (c) approaches are shown. One result of the 10 simulations in aged-diverse approach is shown.

### 503 5.1. Stability of simulation results

504 The aged-diverse approach is stochastic, and the results may differ in multiple simulations. Therefore, it is neces-

505 sary to explore the stability of simulation results to ensure the accuracy of our analysis based on the simulation results.

506 Ten repeated simulations using an aged-diverse approach were conducted, and the profiles of  $H_{di}$ ,  $C_{di}$ ,  $H_{hour}$ ,  $C_{hour}$  are

507 shown in Fig.8,  $HI_k$  and  $CI_k$  distributions shown in Fig.10.

508 The hourly and diurnal profiles in the aged-diverse approach overlap in Fig.8, since the profiles are aggregated

509 by the profiles of 33,222 buildings, stochasticity in the results of different simulations is eliminated. For  $HI_k$  and

510  $CI_k$ , the distributions generated by the ten simulations differ from each other, whereas the forms of the distributions

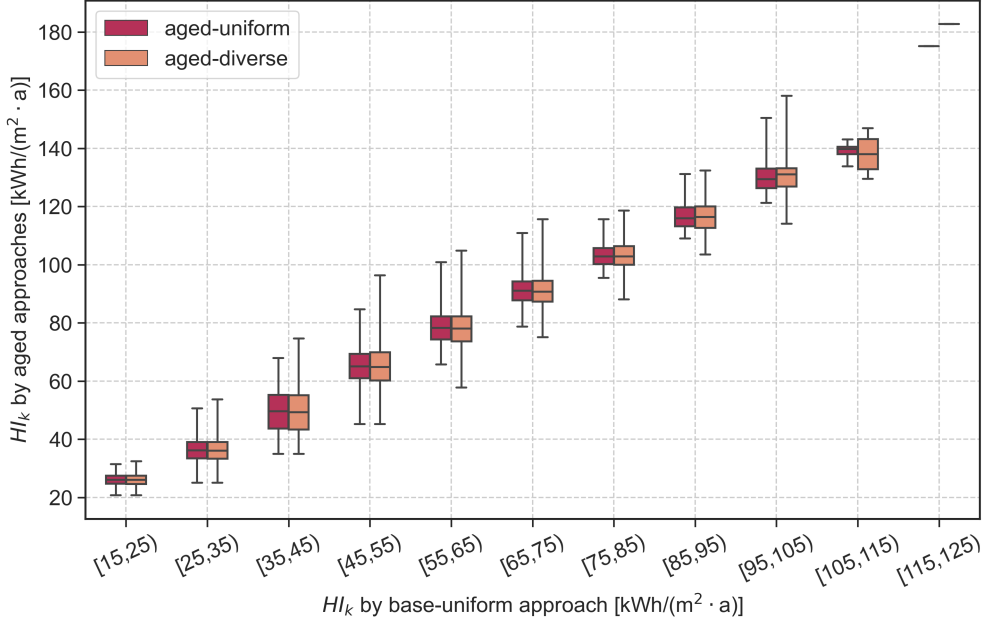


Figure 12: Heating demand intensity  $HI_k$  by aged approaches of buildings categorized by levels of heating demand in base-uniform approach.

511 are similar. The distributions by the aged-diverse approach are quite similar to the distribution by the aged-uniform  
 512 approach because the result of the aged-uniform approach is a special case of the result of the aged-diverse approach.  
 513 Although the U-values of a particular building may vary in different simulations, the population distribution of the  
 514 heating demand of the building stock is stable because of the large number of buildings.

515 The uncertainty in  $H_{ann}$  and  $C_{ann}$  decreases as more buildings are aggregated. The ten repeated simulation results  
 516 of  $H_{ann}$  and  $C_{ann}$  in the aged-diverse approach divided by the total floor area of the building stock are shown in  
 517 Fig.13, compared with  $HI_k$  and  $CI_k$  of an individual building. Considering the uncertainty of the U-values,  $HI_k$  and  
 518  $CI_k$  of each building vary in multiple simulations; however,  $H_{ann}$  and  $C_{ann}$  divided by the total floor area are almost  
 519 unchanged when the entire building stock is aggregated. The coefficients of variation (CV) of the results of the  
 520 ten repeated simulations are compared in Table.7. The CVs of  $H_{ann}$  and  $C_{ann}$  at the urban scale were smaller than  
 521 1% in the repeated simulations and were much smaller than those at the building scale, which means that the total  
 522 heating/cooling demand was stable in repeated simulations for the building stock as large as in the case study.

Table 7: Coefficients of variation (CV) of 10 repeated simulations at different spatial scale.

| Spatial scale | CV of $H_{ann}$ (%) | CV of $C_{ann}$ (%) |
|---------------|---------------------|---------------------|
| Building      | 5.43                | 2.67                |
| Urban         | 0.04                | 0.02                |

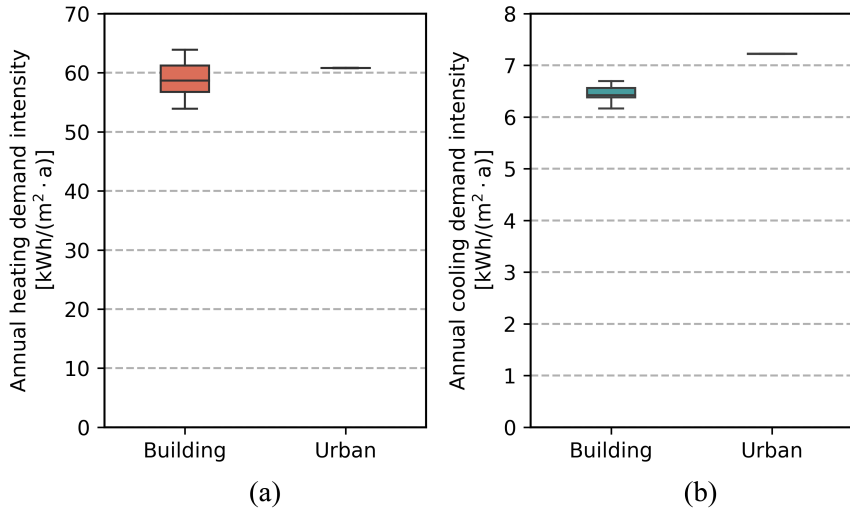


Figure 13: Comparison of annual heating/cooling demand per unit floor area for individual building and the whole building stock. The *Building* demand is represented by the annual demand intensity  $HI_k/CI_k$  of an example building. The *Urban* average demands are the annual total demands  $H_{\text{ann}}/C_{\text{ann}}$  divided by total floor area of the whole building stock.

### 523 5.2. Appropriate U-value models for different UBEM purposes

524 As shown in the results above, aged approaches considering uncertainty in building envelope thermal transmittance  
 525 provide a more accurate depiction of the population distribution of building stock heating/cooling demand. When  
 526 aggregating buildings together, the impact of uncertainty in the building envelope on the aggregated heating/cooling  
 527 demand decreases and converges to the average value.

528 However, the importance of uncertainty in the building envelope thermal performance depends on the purpose and  
 529 context of UBEM. UBEMs can provide a multidimensional assessment of building energy consumption. When using  
 530 UBEM to analyze energy consumption at the district or urban scale, only part of the results will be used, focusing on  
 531 the major problems to be solved. Therefore, it is important to consider the sufficient fidelity of models to ensure both  
 532 the credibility of the results and simplification of the model at the same time.

533 The common applications of UBEM and the corresponding metrics are reviewed: (1) total heating and cooling  
 534 consumption ( $H_{\text{ann}}$  and  $C_{\text{ann}}$ ), (2) profiles of heating and cooling demand ( $H_{\text{hour}}$ ,  $C_{\text{hour}}$ ,  $H_{\text{di}}$  and  $C_{\text{di}}$ , including peak  
 535 load), and (3) distribution or spatial-temporal characteristics of heating and cooling demand ( $HI_k$  and  $CI_k$ ).

536 The total heating and cooling consumption supports the assessment of energy consumption and carbon emissions,  
 537 which provides guidance for stakeholders in formulating an energy transition plan [64]. In evaluating the total heating  
 538 consumption, the uncertainty in building envelope thermal transmittance needs to be considered, as the discrepancy  
 539 between the average U-values of buildings built in each year and the initial U-values is sufficient to reflect the impact  
 540 of uncertainty on heating/cooling demand at the urban scale, whereas the stochasticity in U-values of buildings built  
 541 in the same year could be neglected.

542 Profiles of heating and cooling demands help in energy supply and demand analysis, demand response, and energy

storage system design [65]. Peak heating and cooling loads also aid in the sizing of chillers or boilers in district heating and cooling [66]. However, the discrepancy between the average U-values of buildings built each year and the initial U-values has a greater impact on the profiles than the stochasticity in U-values.

However, there are some applications of UBEM in which the distribution or spatial-temporal characteristics of the heating and cooling demand of building stock [67], such as UBEM calibration, resilience analysis [68] and energy inequality [69] for buildings in the stock. The uncertainty of building envelope thermal transmittance is worth considering to present the diversity of buildings in a real city and may improve the simulation. For such research purposes, the discrepancy between the average U-values of buildings built in each year and the initial U-values needs to be considered to prevent underestimation of U-values. The stochasticity among building envelope thermal transmittances has an impact on the distribution of heating demand distribution, especially for the building stock with a smaller range of heating demand (Fig. 11) or a smaller range of vintage (Fig. 12).

Table.8 summarizes the evaluation metrics and the appropriate model of building envelope thermal transmittance for different UBEM applications. Table.8 gives an answer to research question Q3 to balance the model fidelity and complexity.

Table 8: Comparisons of the evaluation metrics and U-value models for different UBEM applications.

| Evaluation metrics  | Appropriate approach |              | Applications  |
|---|----------------------|--------------|---|
|   | aged-uniform         | aged-diverse |   |
| Annual total demand<br>( $H_{\text{ann}}$ and $C_{\text{ann}}$ )  | ✓                    |              | Evaluation urban heating/cooling demand for energy policies and plans.  |
| Demand profiles at urban scale<br>( $H_{\text{di}}$ , $H_{\text{hour}}$ , $C_{\text{di}}$ and $C_{\text{hour}}$ ) | ✓                    |              | Energy supply and demand analysis;<br>Demand response;<br>Energy storage system design;<br>Boiler/Chiller sizing. |
| Demand distribution<br>(Distribution of $HI_k$ and $CI_k$ )   | ✓*                   | ✓**          | UBEM calibration;<br>Analysis for each building in the stock (resilience, energy inequality and etc.)             |

\* Especially for the population distribution analysis with a wide range of heating demand or vintage.

\*\* Especially for the building stock with a small range of heating demand or a small range of vintage.

## 6. Conclusion

This study designed and implemented a framework to quantify the uncertainty in the thermal transmittance of a building envelope and analyze its impact on the heating/cooling demand at an urban scale. Compared with state-of-the-art building characterization in UBEM, the proposed approaches reflected the diversity of the thermal performance of buildings with higher fidelity. A case study on 33,222 residential buildings in Beijing showed that uncertainty in building envelopes has an impact on the heating/cooling demand of the building stock. The hourly and diurnal profiles,

563 annual heating/cooling demand, and heating/cooling demand distribution were influenced.

564 Considering the uncertainty in the thermal transmittance of buildings introduced by physical factors in real con-  
565 ditions, thermal transmittance follows a right-skewed distribution, which is different from the previous assumption  
566 that thermal transmittance is symmetrically distributed on both sides of the U-values in the design. Accordingly, the  
567 heating/cooling demands of the majority of buildings have increased. Uncertainty in the building envelope thermal  
568 transmittance has an increasing effect on the heating/cooling demand. The uncertainty in the thermal transmittance  
569 of the building envelope had a greater influence on the heating demand than on the cooling demand. Considering  
570 the uncertainty of thermal transmittance, the annual total heating demand increased by 26%, whereas the annual total  
571 cooling demand increased by 13%. In addition, the profiles of the heating/cooling demand considering uncertainty  
572 are different from those obtained using the base-uniform approach. Therefore, the gap between the initial U-values in  
573 design and the real U-value distributions is important to quantify the heating/cooling demand of urban building stock.

574 Uncertainty in thermal transmittance is also worth considering when the distributions of building heating/cooling  
575 demand intensity are indicators in the UBEM. The uncertainty in the thermal transmittance of the building envelope  
576 has a significant impact on the distribution form and dispersion of the heating/cooling demand intensity of the building  
577 stock. The discrepancy between the average U-values of buildings built in different years and the stochasticity in the  
578 U-values of buildings built in the same year are possible causes of uncertainty. The two possible causes proposed  
579 in this study affect the heating/cooling demand of building stock. However, considering the balance of fidelity and  
580 complexity, the discrepancy between the average U-values of buildings built in different years and initial U-values  
581 is sufficient for the evaluation of heating/cooling profiles and annual total demand. For the heating/cooling demand  
582 distribution of the entire building stock, stochasticity has almost no further effect, compared with the distribution that  
583 only considers discrepancy. However, for a building stock with a smaller range of building age or heating demand  
584 intensity, the impact of stochasticity on heating demand distribution may increase and deserve consideration.

585 The results of this study could provide a reference to the cities with similar climate to Beijing, where heating de-  
586 mand is dominant. Furthermore, considering the uncertainty in the thermal transmittance of buildings, the application  
587 of the proposed approaches would be promising for both the improvement of UBEM and energy-related analysis at the  
588 urban scale, such as UBEM calibration and urban building retrofit analysis. The diversified building characterization  
589 considering the uncertainty in building envelope thermal transmittance could serve as a starting point for applications  
590 such as resilience, carbon neutrality, and energy inequality assessment of urban buildings.

## 591 Acknowledgements

592 This publication has been jointly written within the cooperative project “Key technologies and demonstration of  
593 combined cooling, heating and power generation for low-carbon neighbourhoods/buildings with clean energy – Chi-  
594 NoZEN”. The authors gratefully acknowledge the funding support from the Ministry of Science and Technology of  
595 China (MOST project number 2019YFE0104900), and from the Research Council of Norway (NRC project num-

596 ber 304191 - ENERGIX) . The authors would also like to acknowledge the support from Beijing Municipal Natural  
597 Science Foundation of China (Grant number 8222019), Tsinghua-Foshan Innovation Special Fund(TFISF 2021THF-  
598 S0201).

599 **Appendix A. Details in UBEM characterization**

600 The settings of the residential building energy models used in the UBEM are listed in Table.A.1. Most parameters  
601 are based on prototype building models based on actual energy consumption in [60]. The parameters not mentioned  
602 are the default parameters of DeST engine.

Table A.1: System operation and occupant behavior parameters of residential building models in UBEM characterization.

| Parameter                         | Value                                 |
|-----------------------------------|---------------------------------------|
| Indoor temperature range          | 20°C-26°C                             |
| Heating demand calculation period | From Nov. 20th to Mar. 18th next year |
| Heating schedule                  | ON 24 hours a day                     |
| Cooling demand calculation period | From Mar.19th to Nov.19th             |
| Cooling schedule                  | Fig.A.1 (a)(b)                        |
| Occupant sensible heat gain       | 53 W/pers                             |
| Occupant latent heat gain         | 61g <sub>water</sub> /(h·pers)        |
| Occupancy density                 | 0.037 pers/m <sup>2</sup>             |
| Occupancy schedule                | Fig.A.1 (c)(d)                        |
| Light&appliance schedule          | Fig.A.1 (e)                           |
| Light&appliance power density     | 9.3 W/m <sup>2</sup>                  |
| Air change rate                   | 0.5 ACH                               |

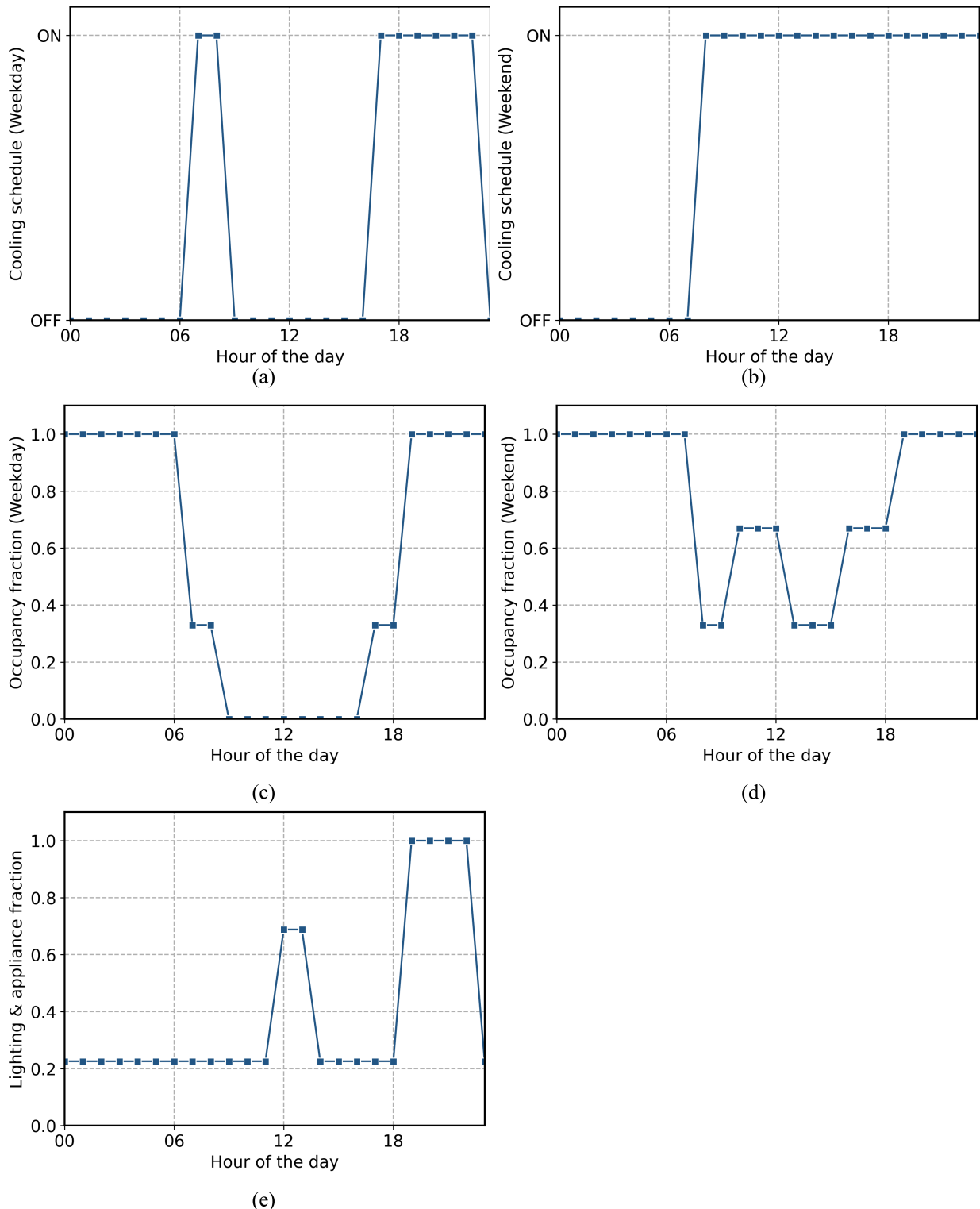


Figure A.1: Prototype default profiles for (a) cooling schedule of weekdays, (b) cooling schedule of weekends, (c) occupancy of weekdays, (d) occupancy of weekends, and (e) lighting and appliance use.

603 **Appendix B. Results of Kolmogorov-Smirnov test**

Table A.2: Results of Kolmogorov-Smirnov test. P-values are listed in the table and asterisks (\*) in parentheses represent significance levels.

|                        | Base-uniform vs. Aged-uniform | Base-uniform vs. Aged-diverse | Aged-uniform vs. Aged-diverse |
|------------------------|-------------------------------|-------------------------------|-------------------------------|
| Distribution of $HI_k$ | 0 (***)                       | 0 (***)                       | $3.4 \times 10^{-4}$ (***)    |
| Distribution of $CI_k$ | 0 (***)                       | 0 (***)                       | 0.83                          |

604 **References**

- 605 [1] U. N. E. Programme, 2020 global status report for buildings and construction: Towards a zero-emission, efficient and resilient buildings and  
construction sector (2020).
- 606 [2] T. Hong, H. Sun, Y. Chen, S. C. Taylor-Lange, D. Yan, An occupant behavior modeling tool for co-simulation, Energy and Buildings 117  
(2016) 272–281.
- 607 [3] N. Abbasabadi, M. Ashayeri, Urban energy use modeling methods and tools: A review and an outlook, Building and Environment 161 (2019)  
106270.
- 608 [4] B. E. R. C. of Tsinghua University, 2021 annual report on china building energy efficiency (2021).
- 609 [5] P. Zhu, D. Yan, H. Sun, J. An, Y. Huang, Building blocks energy estimation (bbee): A method for building energy estimation on district level,  
Energy and Buildings 185 (2019) 137–147.
- 610 [6] C. F. Reinhart, C. C. Davila, Urban building energy modeling—a review of a nascent field, Building and Environment 97 (2016) 196–202.
- 611 [7] U. Ali, M. H. Shamsi, C. Hoare, E. Mangina, J. O'Donnell, Review of urban building energy modeling (ubem) approaches, methods and  
tools using qualitative and quantitative analysis, Energy and Buildings 246 (2021) 111073.
- 612 [8] F. Johari, G. Peronato, P. Sadeghian, X. Zhao, J. Widén, Urban building energy modeling: State of the art and future prospects, Renewable  
and Sustainable Energy Reviews 128 (2020) 109902.
- 613 [9] S. Zhan, Z. Liu, A. Chong, D. Yan, Building categorization revisited: A clustering-based approach to using smart meter data for building  
energy benchmarking, Applied Energy 269 (2020) 114920.
- 614 [10] Y. Q. Ang, Z. Berzolla, S. Letellier-Duchesne, V. Jusiega, C. Reinhart, Ubem. io: A web-based framework to rapidly generate urban building  
energy models for carbon reduction technology pathways, Sustainable Cities and Society (2021) 103534.
- 615 [11] Y. Q. Ang, Z. M. Berzolla, C. F. Reinhart, From concept to application: A review of use cases in urban building energy modeling, Applied  
Energy 279 (2020) 115738.
- 616 [12] N. Buckley, G. Mills, C. Reinhart, Z. M. Berzolla, Using urban building energy modelling (ubem) to support the new european union's green  
deal: Case study of dublin ireland, Energy and Buildings 247 (2021) 111115.
- 617 [13] M. Ferrando, F. Causone, T. Hong, Y. Chen, Urban building energy modeling (ubem) tools: A state-of-the-art review of bottom-up physics-  
based approaches, Sustainable Cities and Society (2020) 102408.
- 618 [14] T. Hong, Y. Chen, X. Luo, N. Luo, S. H. Lee, Ten questions on urban building energy modeling, Building and Environment (2019)  
106508doi:10.1016/j.buildenv.2019.106508.
- 619 [15] A. Peluchetti, G. Guazzi, E. Lucchi, I. Dall'Orto, C. P. López, Criteria for building types selection in preserved areas to pre-assess the building  
integrated photovoltaics solar potential—the case study of como land area, in: IOP Conference Series: Earth and Environmental Science, Vol.  
863, IOP Publishing, 2021, p. 012003.
- 620 [16] E. Lucchi, V. D'Alonzo, D. Exner, P. Zambelli, G. Garegnani, A density-based spatial cluster analysis supporting the building stock analysis  
in historical towns, in: Proceedings of the Building Simulation, 2019, pp. 3831–3838.
- 621 [17] C. Wang, M. Ferrando, F. Causone, X. Jin, X. Zhou, X. Shi, Data acquisition for urban building energy modeling: A review, Building and  
Environment (2022) 109056.

- 638 [18] G. Happle, J. A. Fonseca, A. Schlueter, Impacts of diversity in commercial building occupancy profiles on district energy demand and supply,  
 639 Applied Energy 277 (2020) 115594.
- 640 [19] X. Zhou, J. Ren, J. An, D. Yan, X. Shi, X. Jin, Predicting open-plan office window operating behavior using the random forest algorithm,  
 641 Journal of Building Engineering 42 (2021) 102514.
- 642 [20] X. Zhou, S. Tian, J. An, D. Yan, L. Zhang, J. Yang, Modeling occupant behavior's influence on the energy efficiency of solar domestic hot  
 643 water systems, Applied Energy 309 (2022) 118503.
- 644 [21] B. Jones, P. Das, Z. Chalabi, M. Davies, I. Hamilton, R. Lowe, A. Mavrogianni, D. Robinson, J. Taylor, Assessing uncertainty in housing  
 645 stock infiltration rates and associated heat loss: English and uk case studies, Building and environment 92 (2015) 644–656.
- 646 [22] J. T. Szcześniak, Y. Q. Ang, S. Letellier-Duchesne, C. F. Reinhart, A method for using street view imagery to auto-extract window-to-wall  
 647 ratios and its relevance for urban-level daylighting and energy simulations, Building and Environment 207 (2022) 108108.
- 648 [23] J. Sokol, C. C. Davila, C. F. Reinhart, Validation of a bayesian-based method for defining residential archetypes in urban building energy  
 649 models, Energy and Buildings 134 (2017) 11–24.
- 650 [24] C. Cerezo, J. Sokol, S. AlKhaled, C. Reinhart, A. Al-Mumin, A. Hajiah, Comparison of four building archetype characterization methods in  
 651 urban building energy modeling (ubem): A residential case study in kuwait city, Energy and Buildings 154 (2017) 321–334.
- 652 [25] S. Risch, P. Remmen, D. Müller, Influence of data acquisition on the bayesian calibration of urban building energy models, Energy and  
 653 Buildings 230 (2021) 110512.
- 654 [26] I. De Jaeger, J. Lago, D. Saelens, A probabilistic building characterization method for district energy simulations, Energy and buildings 230  
 655 (2021) 110566.
- 656 [27] W. Tian, Y. Heo, P. De Wilde, Z. Li, D. Yan, C. S. Park, X. Feng, G. Augenbroe, A review of uncertainty analysis in building energy  
 657 assessment, Renewable and Sustainable Energy Reviews 93 (2018) 285–301. doi:10.1016/j.rser.2018.05.029.
- 658 [28] E. Lucchi, Thermal transmittance of historical stone masonry: A comparison among standard, calculated and measured data, Energy and  
 659 Buildings 151 (2017) 393–405.
- 660 [29] M. Andreotti, D. Bottino-Leone, M. Calzolari, P. Davoli, L. Dias Pereira, E. Lucchi, A. Troi, Applied research of the hygrothermal behaviour  
 661 of an internally insulated historic wall without vapour barrier: In situ measurements and dynamic simulations, Energies 13 (13) (2020) 3362.
- 662 [30] E. Lucchi, Thermal transmittance of historical brick masonry: A comparison among standard data, analytical calculation procedures, and in  
 663 situ heat flow meter measurements, Energy and Buildings 134 (2017) 171–184.
- 664 [31] Stochastic energy-demand analyses with random input parameters for the single-family house, Building Simulation 15 (3) (2022) 357–371.  
 665 doi:10.1007/s12273-021-0812-9.  
 666 URL <https://doi.org/10.1007/s12273-021-0812-9>
- 667 [32] F. Domínguez-Muñoz, B. Anderson, J. M. Cejudo-López, A. Carrillo-Andrés, Uncertainty in the thermal conductivity of insulation materials,  
 668 Energy and Buildings 42 (11) (2010) 2159–2168.
- 669 [33] U. Berardi, The impact of aging and environmental conditions on the effective thermal conductivity of several foam materials, Energy 182  
 670 (2019) 777–794.
- 671 [34] S. N. Singh, P. D. Coleman, Accelerated aging test methods for predicting the long term thermal resistance of closed-cell foam insulation, in:  
 672 Center for Polyurethanes Industries Conference, Vol. 15, 2007.
- 673 [35] E. Wegger, B. P. Jelle, E. Sveipe, S. Grynnning, A. Gustavsen, R. Baetens, J. V. Thue, Aging effects on thermal properties and service life of  
 674 vacuum insulation panels, Journal of Building Physics 35 (2) (2011) 128–167.
- 675 [36] H. Simmler, S. Brunner, Vacuum insulation panels for building application: Basic properties, aging mechanisms and service life, Energy and  
 676 buildings 37 (11) (2005) 1122–1131.
- 677 [37] A. Batard, T. Duforestel, L. Flandin, B. Yrieix, Modelling of long-term hygro-thermal behaviour of vacuum insulation panels, Energy and  
 678 Buildings 173 (2018) 252–267.
- 679 [38] X. Shen, L. Li, W. Cui, Y. Feng, Thermal and moisture performance of external thermal insulation system with periodic freezing-thawing,  
 680 Applied Thermal Engineering 181 (2020) 115920.

- 681 [39] E. Lucchi, F. Roberti, T. Alexandra, Definition of an experimental procedure with the hot box method for the thermal performance evaluation  
682 of inhomogeneous walls, *Energy and Buildings* 179 (2018) 99–111.
- 683 [40] B. Tejedor, E. Lucchi, D. Bienvenido-Huertas, I. Nardi, Non-destructive techniques (ndt) for the diagnosis of heritage buildings: traditional  
684 procedures and futures perspectives, *Energy and Buildings* (2022) 112029.
- 685 [41] R. F. De Masi, S. Ruggiero, G. P. Vanoli, Multi-layered wall with vacuum insulation panels: Results of 5-years in-field monitoring and  
686 numerical analysis of aging effect on building consumptions, *Applied Energy* 278 (2020) 115605.
- 687 [42] F. Stazi, F. Tittarelli, G. Politi, C. Di Perna, P. Munafò, Assessment of the actual hygrothermal performance of glass mineral wool insulation  
688 applied 25 years ago in masonry cavity walls, *Energy and Buildings* 68 (2014) 292–304.
- 689 [43] B. Barahona, R. Buck, O. Okaya, P. Schuetz, Detection of thermal anomalies on building façades using infrared thermography and supervised  
690 learning, in: *Journal of Physics: Conference Series*, Vol. 2042, IOP Publishing, 2021, p. 012013.
- 691 [44] N. Bayomi, S. Nagpal, T. Rakha, J. E. Fernandez, Building envelope modeling calibration using aerial thermography, *Energy and Buildings*  
692 233 (2021) 110648.
- 693 [45] Z. Deng, Y. Chen, J. Yang, Z. Chen, Archetype identification and urban building energy modeling for city-scale buildings based on gis  
694 datasets, *Building Simulation* (2022) 1–13.
- 695 [46] R. Buffat, A. Froemelt, N. Heeren, M. Raubal, S. Hellweg, Big data gis analysis for novel approaches in building stock modelling, *Applied  
696 Energy* 208 (2017) 277–290.
- 697 [47] Y. Chen, Z. Deng, T. Hong, Automatic and rapid calibration of urban building energy models by learning from energy performance database,  
698 *Applied Energy* 277 (2020) 115584.
- 699 [48] M. Röck, M. R. M. Saade, M. Balouktsi, F. N. Rasmussen, H. Birgisdottir, R. Frischknecht, G. Habert, T. Lützkendorf, A. Passer, Embodied  
700 ghg emissions of buildings—the hidden challenge for effective climate change mitigation, *Applied Energy* 258 (2020) 114107.
- 701 [49] B.-H. Choi, J.-S. Kang, The thermal performance of building insulation materials according to long-term aging, *Korean Journal of Air-  
702 Conditioning and Refrigeration Engineering* 25 (11) (2013) 617–623.
- 703 [50] P. Hall, J. Strutt, Probabilistic physics-of-failure models for component reliabilities using monte carlo simulation and weibull analysis: a  
704 parametric study, *Reliability Engineering & System Safety* 80 (3) (2003) 233–242.
- 705 [51] B. Ward, A. Selby, S. Gee, D. Savic, Deterioration modelling of small-diameter water pipes under limited data availability, *Urban Water  
706 Journal* 14 (7) (2017) 743–749. doi:10.1080/1573062X.2016.1254252.
- 707 [52] T. S. Betz, M. N. Grussing, L. B. Bartels, Optimizing markov probabilities for generation of a weibull model to characterize building  
708 component failure processes, *Journal of Performance of Constructed Facilities* 35 (6) (2021) 04021077.
- 709 [53] X. Kang, D. Yan, X. Xie, J. An, Z. Liu, Co-simulation of dynamic underground heat transfer with building energy modeling based on  
710 equivalent slab method, *Energy and Buildings* 256 (2022) 111728.
- 711 [54] D. Yan, J. Xia, W. Tang, F. Song, X. Zhang, Y. Jiang, Dest—an integrated building simulation toolkit part i: Fundamentals, in: *Building  
712 Simulation*, Vol. 1, Springer, 2008, pp. 95–110.
- 713 [55] D. Yan, X. Zhou, J. An, X. Kang, F. Bu, Y. Chen, Y. Pan, Y. Gao, Q. Zhang, H. Zhou, et al., DeST 3.0: A new-generation building performance  
714 simulation platform, *Building Simulation* doi:10.1007/s12273-022-0909-9.
- 715 [56] T. Hong, Y. Jiang, A new multizone model for the simulation of building thermal performance, *Building and environment* 32 (2) (1997)  
716 123–128.
- 717 [57] T. Hong, J. Zhang, Y. Jiang, Iisabre: An integrated building simulation environment, *Building and Environment* 32 (3) (1997) 219–224.
- 718 [58] T. H. Kolbe, G. Gröger, L. Plümer, Citygml: Interoperable access to 3d city models, in: *Geo-information for disaster management*, Springer,  
719 2005, pp. 883–899.
- 720 [59] A. Malhotra, M. Shamovich, J. Frisch, C. van Treeck, Urban energy simulations using open citygml models: A comparative analysis, *Energy  
721 and Buildings* 255 (2022) 111658.
- 722 [60] C. Gui, D. Yan, S. Guo, J. An, Development of prototype building model in beijing based on actual energy consumption, in: *The International  
723 Symposium on Heating, Ventilation and Air Conditioning*, Springer, Singapore, 2019, pp. 1187–1196.

- 724 [61] JGJ 26-86, Energy conservation design standard for new heating residential buildings (1986).
- 725 [62] JGJ 26-95, Energy conservation design standard for new heating residential buildings (1995).
- 726 [63] JGJ 26-2010, Design standard for energy efficiency of residential buildings in severe cold and cold zones (2010).
- 727 [64] P. Caputo, G. Costa, S. Ferrari, A supporting method for defining energy strategies in the building sector at urban scale, *Energy Policy* 55 (2013) 261–270.
- 729 [65] A. Walker, S. Kwon, Design of structured control policy for shared energy storage in residential community: A stochastic optimization approach, *Applied Energy* 298 (2021) 117182.
- 731 [66] J. An, D. Yan, T. Hong, K. Sun, A novel stochastic modeling method to simulate cooling loads in residential districts, *Applied Energy* 206 (2017) 134–149.
- 733 [67] B. Howard, L. Parshall, J. Thompson, S. Hammer, J. Dickinson, V. Modi, Spatial distribution of urban building energy consumption by end use, *Energy and Buildings* 45 (2012) 141–151.
- 735 [68] B. Dong, Y. Liu, H. Fontenot, M. Ouf, M. Osman, A. Chong, S. Qin, F. Salim, H. Xue, D. Yan, et al., Occupant behavior modeling methods for resilient building design, operation and policy at urban scale: A review, *Applied Energy* 293 (2021) 116856.
- 737 [69] Y. Zhang, S. Hu, D. Yan, S. Guo, P. Li, Exploring cooling pattern of low-income households in urban china based on a large-scale questionnaire survey: A case study in beijing, *Energy and Buildings* 236 (2021) 110783.